

# The Composition of the Atmosphere of Jupiter

F. W. Taylor

*Oxford University*

S. K. Atreya

*University of Michigan*

Th. Encrenaz

*Observatoire de Paris, Meudon*

D. M. Hunten

*University of Arizona*

P. G. J. Irwin

*Oxford University*

T. C. Owen

*University of Hawaii*

## 4.1 INTRODUCTION

Modern studies of the composition of Jupiter's atmosphere date back to the mid-nineteenth century, when the near-infrared spectrum of the planet was viewed by Rutherford (1863) using diffraction gratings of his own manufacture. He discovered features that remained unidentified until 1932, when Wildt showed that the unknown spectral lines were due to ammonia and methane. In later years, building on the original insight of Jeffreys (1923, 1924), Wildt and others went on to note that the low density of Jupiter and the presence of these hydrogen-rich compounds in the atmosphere were consistent with a bulk composition similar to that of the Sun, that is, primarily hydrogen.

Despite its expected high abundance, hydrogen is difficult to observe because of the absence of a dipole spectrum. Herzberg predicted in 1938 that the quadrupole absorption lines might be observable, and the (3-0) lines at 815 and 827 nm were eventually detected by Kiess *et al.* (1960) and the (4-0) band near 637 nm by Spinrad and Trafton (1963). Although the presence of around 10% of helium had been anticipated on cosmogonical grounds, it was not detected directly until the *Pioneer 10* encounter in 1973, when the ultraviolet photometer measured the 58.40 nm resonance line (Judge and Carlson 1974). Since then, progress in detecting additional species, some present in only very small amounts, has been rapid, with contributions from both ground based and space borne instruments.

## 4.2 SOLAR ABUNDANCE AND NUCLEATION MODELS

Before 1980, the traditional approach to obtaining a first-order model of the composition of Jupiter was to assume that the planet as a whole has the same composition as the Sun, with which, like all of the planets, it has a common origin in the protosolar nebula. The large mass of Jupiter, and its formation in a sufficiently low temperature region, was invoked to infer that the planet had apparently retained a solar proportion of even the lightest element, hydrogen.

The atmosphere of Jupiter is evidently well-mixed to a great depth, and the reasonable assumption that chemical equilibrium is attained in the hot interior leads to the expectation that the common elements are all fully reduced by combination with hydrogen. Thus, carbon, nitrogen, oxygen and sulfur, for example, should be represented in the atmosphere as methane (CH<sub>4</sub>), ammonia (NH<sub>3</sub>), water (H<sub>2</sub>O), and hydrogen sulfide (H<sub>2</sub>S). The fact that these species do appear as the most abundant after hydrogen and helium, plus the near-solar ratio between the two bulk constituents, was thought for a time to validate the solar abundance model. Table 4.1 shows a recent example of what the composition of Jupiter would be if it was determined from such a model, based on the work of Anders and Grevesse (1989).

For understanding the composition of Jupiter, solar models are a useful starting point, but it has become increasingly clear since the time of the *Voyager* missions that Jupiter and the Sun do not have identical elemental abundances. In seeking to study the differences, we must keep

**Table 4.1.** A model for the composition of Jupiter based on a “solar” abundance of elements (Anders and Grevesse 1989).

Gas	Volume Mixing Ratio (vmr)
H <sub>2</sub>	0.835
He	0.16
H <sub>2</sub> O	0.0015
CH <sub>4</sub>	0.0007
NH <sub>3</sub>	0.00018
Ne	0.00019
H <sub>2</sub> S	0.000031
Ar	6.1 ppm
Kr	1.5 ppb
Xe	0.07 ppb

in mind that our understanding of the current, protosolar (i.e., at the time of solar system formation), and primordial (i.e., before any star formation) composition of the Sun, as well as that of Jupiter, continues to evolve, with new measurements and interpretations appearing regularly. Since the Anders and Grevesse (1989) compilation shown in Table 4.1, the abundances of C, N, and O have been revised by Holweger (2001) and still more recently by Prieto *et al.* (2001, 2002), while new values for the abundances of Ar, Kr and Xe have been given by Grevesse and Sauval (1998). It remains to be seen how significant these revisions are; in this review we will use Table 4.1 as a reference point for solar composition as this has been adopted as the standard in recent key publications to which we will refer.

At the time of the first Jupiter book, the solar-based model for the composition of Jupiter by Lewis (1969) was widely used. Lewis’s solar values for the 10 most abundant molecules were all within a factor of about 2 of the modern solar model shown in Table 4.1, and some much closer. These differences represent a reasonable upper limit on the uncertainty in the solar abundances, and since the most recent values for Jupiter show larger differences than this, they evidently demand a new paradigm for the formation of the planet. Current thinking centers on the so-called “nucleation” theory, first introduced by Mizuno (1980) and later developed by several authors (e.g., Pollack *et al.* 1996). This involves the formation of an initial icy core with a mass of about 12  $M_E$ , where  $M_E$  is the present mass of the Earth, with a gravity field large enough to accrete the surrounding protosolar nebula, mostly composed of hydrogen and helium, with additional solid planetesimals.

Such a scenario has an immediate consequence for the abundance ratios expected to be measured in the planet. Present-day Jupiter has a mass of 318  $M_E$ , of which 12  $M_E$  comprises a heavy-element core according to the authors cited above. If the additional 306  $M_E$  accreted by the core had solar composition it would contain heavy elements (that is, everything heavier than helium) as about 2% of its total mass, i.e., 6  $M_E$ . This makes a total of 18  $M_E$  in heavy elements, for an enrichment of about a factor of 3 relative to solar, which is approximately consistent with the most recent observations. In a more detailed treatment of the nucleation model by Guillot (1999; see also Chapter 3 by Guillot *et al.*) the formation of an initial icy core puts the total mass of heavy elements in the range between 11 and 42  $M_E$ . Assuming general mixing after the gas in-fall phase, this implies

an enrichment with respect to solar abundances by a factor between 2 and 7 for all heavy elements relative to hydrogen.

Thus we see that the apparent overabundance, relative to the Sun, of heavy elements observed in Jupiter lends general support to the nucleation model for the formation of the planet. However, a more detailed interpretation of the composition measurements in terms of global abundances must take into account a number of poorly understood processes taking place on Jupiter itself. These include condensation to form clouds of different compositions over a wide vertical range; non-equilibrium chemistry and, in the upper atmosphere, photochemistry; fractionation and sequestration in the deep interior and core of Jupiter; and the influx, after the initial formation of the planet and continuing to this day, of material in the form of comets, meteorites and dust. All of these factors can be expected to modify substantially the composition of the observable atmosphere, by which we mean the part above a pressure of around 20 bars, which represents the maximum depth sounded by the *Galileo* entry probe and remote sensing at all but the longest radio wavelengths. Vertical and horizontal variations in the mixing ratios of key species like water vapor and ammonia are to be expected, and have been observed. With these difficulties in mind, the question of what tentative conclusions may nevertheless be drawn from the existing measurements about the formation and evolution of Jupiter is considered briefly later in this chapter and in more detail in Chapter 2 by Lunine *et al.*

### 4.3 MEASUREMENTS OF COMPOSITION

The gases found in the atmosphere of Jupiter generally have distinct spectral features, which have been used to determine their abundances from remotely sensed measurements. From the ultraviolet, through the visible to approximately 3.5  $\mu\text{m}$ , the near-infrared spectrum of the planet is dominated by reflected sunlight, scattered by cloud particles and suspended aerosols in the atmosphere, and also by Rayleigh scattering from the gas molecules themselves at the shorter wavelengths. The mid-infrared part of the spectrum begins at about 3.5  $\mu\text{m}$ , where thermal emission starts to dominate over reflected sunlight. By 5  $\mu\text{m}$ , the latter contributes typically only a few percent of the flux, although this varies considerably with cloud cover. The region of the jovian spectrum from about 4 to 6  $\mu\text{m}$  is an atmospheric “window” at the center of which the gaseous opacity is so low that, in the absence of clouds, relatively intense thermal radiation from pressure levels as deep as 5 to 8 bars may be observed. There is no comparable window region at longer wavelengths until the microwave and radio regions are reached, so the rest of the mid and far-infrared spectrum is dominated by emission from depths no greater than 1 or 2 bars in pressure.

The visible and parts of the near-infrared spectrum of Jupiter have been observed for many years by terrestrial telescopes and airborne observatories, and more recently the range and sensitivity have been extended by the Hubble Space Telescope (HST) and the Infrared Space Observatory (ISO). Although much was learned from Earth-based telescopes, some of the most dramatic advances in our understanding of Jupiter followed the rapid flypast of the planet by the *Pioneer* probes in the early 70s and the more

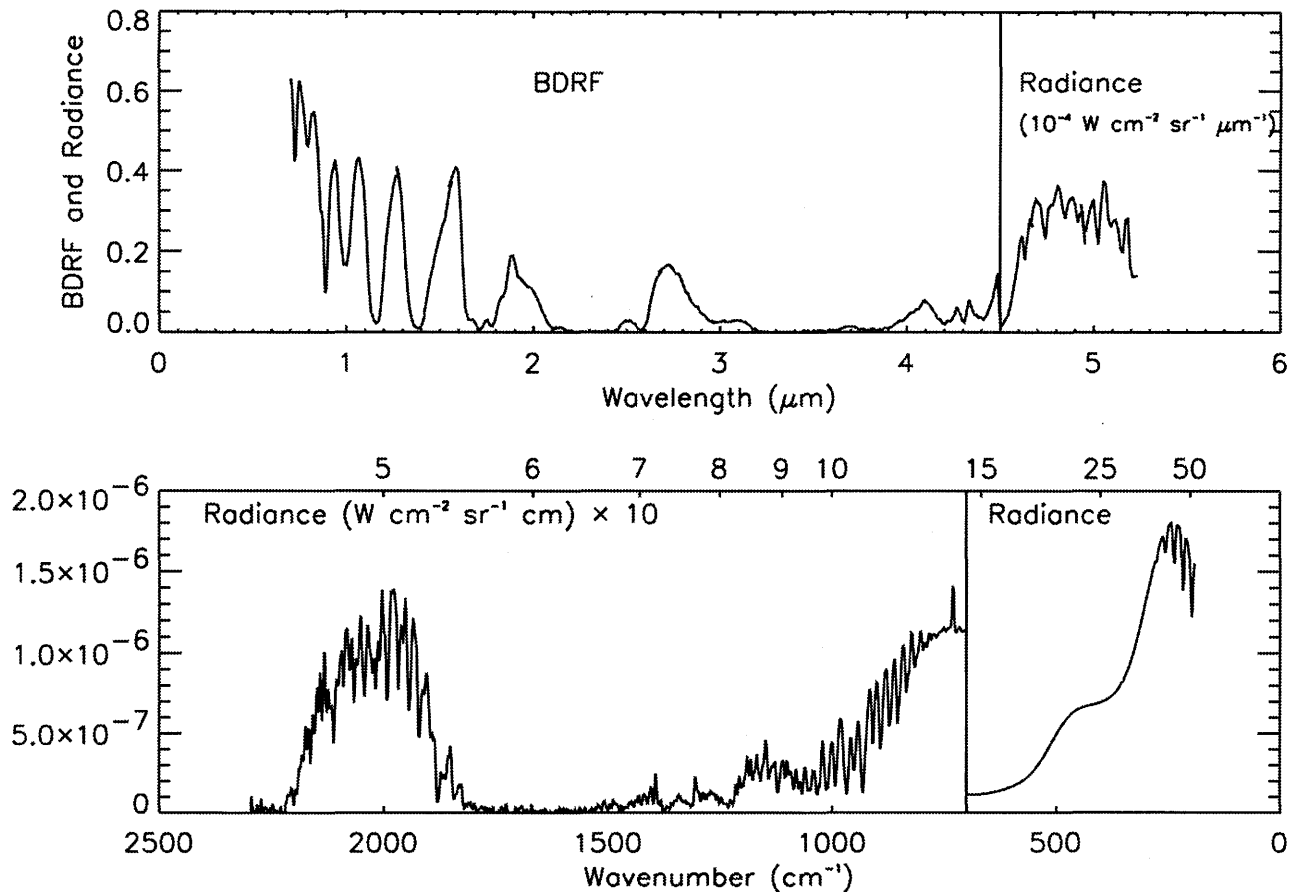


**Figure 4.1.** *Galileo* NIMS (0.7–5.2  $\mu\text{m}$ , top) and *Voyager* IRIS (4.5–55  $\mu\text{m}$ , below) spectra of similar brightness hot-spot regions on Jupiter (Irwin 1999). Note the changes in scale at the vertical line from bi-directional reflectivity function (BDRF) to radiance (in units of  $\mu\text{W cm}^{-2} \text{sr}^{-1} \mu\text{m}^{-1}/100$ ) in the upper plot, and from radiance  $\times 10$  to radiance (in units of  $\text{W cm}^{-2} \text{sr}^{-1} \text{cm}$ ) in the lower plot.

advanced *Voyager* probes at the end of that decade. *Galileo* arrived at Jupiter on December 7, 1995 and deployed the first jovian atmospheric entry probe before becoming the first artificial satellite of Jupiter. The orbiter's remote sensing instruments made systematic observations of the jovian atmosphere and the surfaces of the Galilean moons for over five years. The probe made the first, and for the foreseeable future the only, directly sampled measurements of the composition during its descent through the atmosphere, also on December 7, 1995.

For atmospheric observations, the *Voyager* spacecraft carried the Imaging Science Subsystem (ISS), the Ultraviolet Spectrometer (UVS), the Photopolarimeter (PPS), and the Infrared Interferometer Spectrometer (IRIS).

The last was a Fourier Transform spectrometer that recorded the thermal infrared spectrum from 150–2500  $\text{cm}^{-1}$  (4.8 to 50  $\mu\text{m}$ ) at a resolution of 4.3  $\text{cm}^{-1}$ . The *Galileo* orbiter carried the Solid State Imager (SSI, Belton *et al.* 1996), the Photo-Polarimeter Radiometer (PPR, Orton *et al.* 1996), and the Near Infrared Mapping Spectrometer (NIMS, Carlson *et al.* 1992, 1996). The NIMS instrument covered the range 0.7–5.2  $\mu\text{m}$  at a resolution of 0.0125  $\mu\text{m}$  below 1  $\mu\text{m}$ , and 0.025  $\mu\text{m}$  above, using a grating dispersing a spectrum on to 17 discrete detectors. NIMS had lower spectral resolution, but higher spatial resolution, than IRIS. A typical spectrum of a hot spot (a region of relatively low

cloud cover that appears bright in the spectral window at 5  $\mu\text{m}$ ) as observed by both NIMS and IRIS from 0.7 to 50  $\mu\text{m}$  is shown in Figure 4.1. The pressure at the peak of the calculated transmission weighting functions, a measure of the depth from which most of the observed radiation originates, is plotted in Figure 4.2.

The *Galileo* probe used a quadrupole mass spectrometer to return data on a range of constituents in the jovian atmosphere between pressure levels of 0.51 and 21.1 bars (Niemann *et al.* 1998). It also carried a dedicated helium abundance detector, an optical interferometer that measured the refractive index of the jovian atmosphere very precisely from 2 to 12 bar pressure levels (von Zahn *et al.* 1998). Additional compositional information was obtained from the Net Flux Radiometer, Nephelometer, and Atmospheric Structure instruments, and from measurements of the rate of attenuation with depth of the probe radio uplink. The probe instruments got hotter during their descent than had been anticipated, and the data have required careful analysis to obtain reliable results. It also has to be kept in mind that a single probe cannot characterize the composition everywhere in an inhomogeneous atmosphere. Simultaneous thermal infrared imaging from the Earth showed that the probe entered the atmosphere in one of the 5- $\mu\text{m}$  hot spots, where low cloud cover is expected to be accompanied by relatively low volatile abundances.

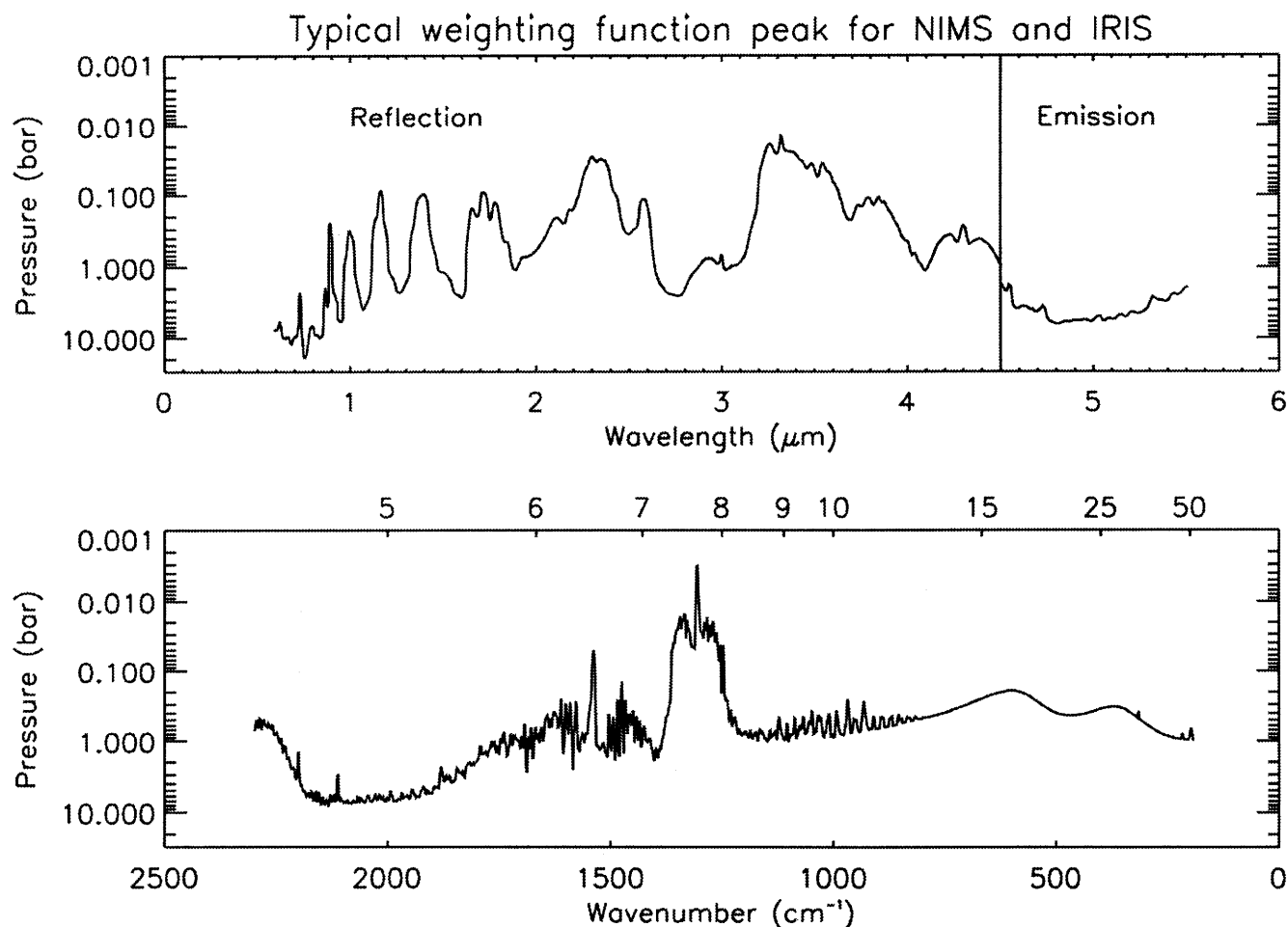


Figure 4.2. Reflection (two-way) and emission (longward of 4.5  $\mu\text{m}$ ) weighting function peak pressure vs. wavelength for the NIMS (top) and IRIS 5  $\mu\text{m}$  spectra. From Irwin (1999).

#### 4.3.1 Observed Molecular Abundances

Table 4.2 presents nominal values for the global mean abundances of the most common species known to be present in Jupiter's atmosphere. Obviously, caution is required in extrapolating from a very limited data set to global mean values and, except for hydrogen and helium, the latter should be regarded as still quite uncertain. In particular, for water vapor the best value we can infer for the global mean from the available measurements is almost certainly a lower limit. Nevertheless, it can be seen from comparisons between Tables 4.1 and 4.2 that significant differences apparently exist between a solar model and the observations.

Just how significant these differences are depends of course on the uncertainties in the values in each table. These cannot be specified precisely because they arise not only from experimental error, which can be estimated, but also from the problem that at least some of the species listed are variable with height and globally due to condensation, vertical transport, chemical production and/or removal. The actual distributions and vertical profiles that result are complicated and variable, being associated with a remarkably diverse and dynamic global meteorology. They are subject to only a very tentative understanding at the present time,

which will be further discussed in the sections on the individual species below. Photochemistry is a particularly important factor in the stratosphere, and additional species not listed in Table 4.2 (for example,  $\text{C}_2\text{H}_6$ ,  $\text{C}_2\text{H}_2$ , and other hydrocarbons, derived photochemically from methane) are present in significant quantities, especially above the 1 mb level (see below and Chapter 7 by Moses *et al.*).

#### *Hydrogen, Deuterium and Helium*

As already noted, hydrogen was first detected in Jupiter through its quadrupole vibrational transitions in the visible part of the spectrum. Later, the rotational quadrupole transitions S(1) and S(0) at 17 and 28  $\mu\text{m}$  respectively, and the pressure-induced rotational spectrum in the far-infrared, were also identified. Measurements of the latter by *Voyager* IRIS were used by Gautier *et al.* (1981) to determine an  $\text{H}_2$  mole fraction of  $0.897 \pm 0.030$  in Jupiter. The analysis assumed that the spectrum was due to  $\text{H}_2\text{-H}_2$  and  $\text{H}_2\text{-He}$  collisions only, i.e., that helium made up the bulk of the remaining 10% or so of the atmosphere. The helium abundance was later measured directly by the *Galileo* probe mass spectrometer, and a value of  $0.136 \pm 0.003$  was obtained for the volume mixing ratio (vmr) (Niemann *et al.* 1998). The

**Table 4.2.** Nominal global mean values for the mixing ratios by volume (mole fractions) of the principal constituents of the troposphere of Jupiter, as inferred from the available measurements. See text for a discussion of the uncertainties in these numbers.

Species	Volume Mixing Ratio
Hydrogen, H <sub>2</sub>	0.86
Helium, He	0.136
Methane, CH <sub>4</sub>	0.0018
Ammonia, NH <sub>3</sub>	0.0007
Water, H <sub>2</sub> O	>0.0005
Hydrogen sulfide, H <sub>2</sub> S	77 ppm
Neon, Ne	20 ppm
Argon, Ar	16 ppm
Hydrogen deuteride, HD	15 ppm
Phosphine, PH <sub>3</sub>	0.5 ppm
Deuterated methane, CH <sub>3</sub> D	0.3 ppm
Krypton, Kr	7.6 ppb
Carbon monoxide, CO	0.75 ppb
Xenon, Xe	0.76 ppb
Germane, GeH <sub>4</sub>	0.6 ppb
Arsine, AsH <sub>3</sub>	0.2 ppb

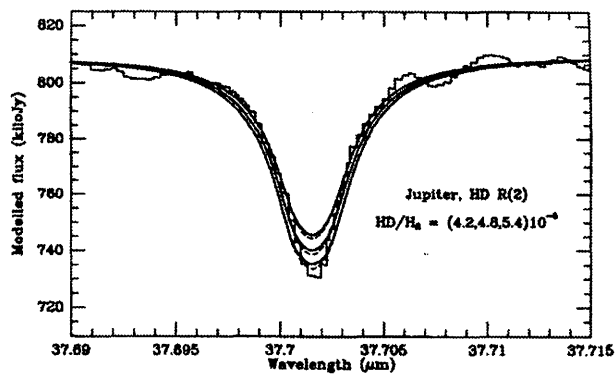


**Figure 4.3.** The R(2) rotational line of HD in Jupiter as observed by ISO-SWS (Lellouch *et al.* 2001).

result from the helium abundance detector on the probe was the same at  $0.1359 \pm 0.0027$  (von Zahn *et al.* 1998). Inverting the argument, this implies an H<sub>2</sub> mole fraction of 0.865, which is the currently accepted value.

Deuterated hydrogen, HD, was first detected through its vibrational transitions in the visible range (Trauger *et al.* 1973). The R(2) and R(3) rotational transitions have been detected more recently with the short-wavelength spectrometer of the Infrared Space Observatory (Encrenaz *et al.* 1996; Lellouch *et al.* 2001; Fig. 4.3). The use of these and other data in the determination of the D/H ratio is discussed below.

#### Methane and Deuterated Methane

Methane is the most abundant species in the upper jovian troposphere after hydrogen and helium, accounting for approximately 0.2% of the molecular abundance. (The most abundant species in the troposphere as a whole is probably water vapor, which is expected to have a higher global mixing ratio than methane in the deep troposphere, although this has yet to be observed.) Methane does not condense at

the temperatures found on Jupiter, and is chemically stable except in the upper atmosphere ( $p < 1$  mbar), where it is dissociated by solar ultraviolet radiation and, at high latitudes, by precipitating energetic particles (see Chapter 7). It is expected therefore to be well-mixed below the region of photochemical activity, and the *Galileo* probe value of  $2.0 \pm 0.15 \times 10^{-3}$  for the volume mixing ratio or vmr (Niemann *et al.* 1998) should apply throughout the troposphere.

Spectral features of deuterated methane (CH<sub>3</sub>D) in the  $\nu_2$  band near 5  $\mu\text{m}$  were first detected in ground-based spectra and used to infer a vmr of  $5 (+3/-2) \times 10^{-7}$  (Beer and Taylor 1978). Kunde *et al.* (1982) obtained  $(3.5 \pm 1.1) \times 10^{-7}$  from the *Voyager* IRIS measurements of the same band, and a reanalysis by Carlson *et al.* (1993) revised this estimate upwards to  $(4.5 \pm 1.6) \times 10^{-7}$ . Irwin *et al.* (1998) used the lower-resolution *Galileo* NIMS spectra to infer a slightly higher CH<sub>3</sub>D vmr of  $(4.9 \pm 0.2) \times 10^{-7}$ . The  $\nu_6$  band of CH<sub>3</sub>D at 8.6  $\mu\text{m}$  was measured using ISO-SWS by Lellouch *et al.* (2001), who found a vmr of  $(1.6 \pm 0.5) \times 10^{-7}$ . Since CH<sub>3</sub>D is unlikely to be variable in the region of the atmosphere to which these measurements pertain, the error bars in some or all of these results are probably underestimated.

#### Ammonia

Along with methane, water vapor and neon, ammonia belongs to a subset of relatively abundant minor constituents in the jovian atmosphere, those with global mean mixing ratios of the order of one part per thousand. Like water, ammonia has a rather complicated vertical distribution, since, unlike methane or neon, ammonia participates in cloud formation in the troposphere (see Chapter 5 by West *et al.* for a full discussion). In a chemical equilibrium model with a solar abundance of elements, it combines with hydrogen sulfide to produce ammonium hydrosulfide (NH<sub>4</sub>SH). This condenses at about 210 K, corresponding to a pressure level of about 2.2 bars, while the residual NH<sub>3</sub> condenses in the upper troposphere, where clouds of ammonia ice crystals are formed at pressures of around 0.7 bars (Atreya *et al.* 1999). Above the tropopause, the vertical profile of ammonia is further depleted by dissociation under the influence of solar UV radiation and energetic particle precipitation.

Features due to gaseous ammonia are present in the *Voyager* IRIS spectra in the ranges 200–260  $\text{cm}^{-1}$ , 700–1200  $\text{cm}^{-1}$  and in the 5  $\mu\text{m}$  window (Conrath and Gierasch 1986). Radiation in the first two emanates from pressures less than about 1.5 bars while the 5  $\mu\text{m}$  measurements probe to much deeper levels (Figure 4.2). In order to fit observations at all of the wavelengths simultaneously, Carlson *et al.* (1993) found that the ammonia mixing ratio must not only decrease with height, but it must also be sub-saturated above the condensation level. This is consistent with observations at centimeter wavelengths by de Pater and Massie (1985).

Estimates of the abundance of ammonia at deeper levels, below the NH<sub>4</sub>SH cloud, can be obtained from observations of thermal emission at far-IR, microwave and radio frequencies. From IRIS observations at 30–50  $\mu\text{m}$ , Marten *et al.* (1981) infer a vmr of  $4.4 \times 10^{-4}$  at several bars pressure, decreasing to  $1.3 \times 10^{-4}$  near the 1 bar level. This may be compared to *Voyager* radio occultation measurements from 1 to 0.3 bar, where the abundance at 1 bar is  $2.21 \times 10^{-4}$

(Lindal *et al.* 1981), and the analysis of the near-infrared ammonia absorption features in the *Galileo* NIMS spectra by Irwin *et al.* (1998), who found the ammonia vmr between the  $\text{NH}_4\text{SH}$  and  $\text{NH}_3$  cloud decks to be  $1.7 \times 10^{-4}$ . Fouchet *et al.* (2000) showed that different  $\text{NH}_3$  vertical distributions are found inside and outside the hot spots, with a lower mixing ratio inside the hot spots (Figure 4.4).

The *Galileo* probe mass spectrometer had difficulties in measuring the abundance of ammonia accurately owing to adsorption on the inlet pipes. However, laboratory studies based on the GPMS engineering unit have led to an estimate of  $7.1 \pm 3.2 \times 10^{-4}$  for the  $\text{NH}_3$  vmr in the 8.6–12.0 bar region (Wong *et al.* 2002, Atreya *et al.* 2002). The communication uplink from the probe was at a frequency of 1387 MHz (21.6 cm), which is attenuated by ammonia absorption. This attenuation was observed as it increased with depth, allowing a further determination of the ammonia profile (Folkner *et al.* 1998). In the hot spot region through which the probe descended, the ammonia vmr was found to be approximately  $3.5 \times 10^{-4}$  at 5 bar increasing to 6 to  $8 \times 10^{-4}$ , consistent with GPMS, at pressures greater than approximately 10 bar. The net flux radiometer on the probe was also sensitive to ammonia absorption. From the NFR data, Sromovsky *et al.* (1998) inferred a vmr of  $2.5 \times 10^{-4}$  at pressures greater than 5 bars, falling to approximately  $1.5 \times 10^{-4}$  at 2.5 bars and then declining more rapidly with height. The derived ammonia vmr profiles from all of these studies are summarized in Figure 4.4.

de Pater *et al.* (2001) have examined the compatibility between the *Galileo* probe and ground-based microwave data in terms of the global mean abundance of ammonia. If the probe measurements are taken to be representative of the whole planet, then modifying the microwave profile (solid line in Figure 4.4) to fit the probe data at  $p > 5$  bars (star symbols) requires the former to compensate with much lower ammonia mixing ratios above 2 bars, bringing it closer to the ISO profiles (dot-dashed lines). While it is encouraging to be able to bring very different types of observations into tentative agreement in this way, it raises the interesting but unsolved question of what may be depleting ammonia on Jupiter in the region around 2 bars, where vigorous vertical mixing applies, along with temperatures much too high for condensation of pure ammonia. The near-coincidence with the level of expected formation of  $\text{NH}_4\text{SH}$  clouds is a tempting explanation, but de Pater *et al.* (2001) note that, for consistency with the known sulfur abundance, each molecule of  $\text{H}_2\text{S}$  would have to combine with about 10 molecules of  $\text{NH}_3$ .

As the profiles of Fouchet *et al.* (2000) show, the abundances of ammonia in the middle and upper atmosphere, where condensation occurs, are modified by dynamics in a manner similar to the effect on water vapor discussed in the following section. Most of the values discussed above refer primarily to the downwelling regions, i.e., the belts, where the probe entered and where spectroscopic measurements are possible. These are relatively depleted in condensates, particularly ammonia and water, and higher values would be expected in the upwelling, cloudy zones, where measurements are lacking. Also, it would be naïve to assume that all belts, or all zones, or all parts of an individual belt or zone, have the same mixing ratio profiles for the condensable species.

### Water Vapor

A solar abundance of oxygen would correspond to a significantly larger mixing ratio for water vapor than was observed by either Earth-based remote sensing or the *Galileo* probe. The remarkable dryness of the jovian atmosphere inferred from these results has been described as a major mystery, some reports going so far as to say that theories of the origin of the solar system must be revised as a result. In fact, it had long been realised that the dark belts, which are a prominent part of the quasi-permanent cloud structure, correspond to the downwelling branches of planetary-scale convection cells driven by the internal heat source within Jupiter. These are depleted in volatiles of many kinds by passing through the condensation temperatures at various levels as they cool while rising. This produces the cloud layers, which are thick in the zones and thinner, sometimes nearly absent, in the belts. The remote sensing measurements are all biased towards the belts, in particular the hot spots which are their most cloud-free parts, simply because that is where most of the infrared signal originates in the spectral regions where water and other species are observed. Had the probe entered one of the cloudy zones which mark the upwelling branches, it would have undoubtedly encountered much moister air.

From the *Voyager* IRIS hot spot spectra, Kunde *et al.* (1982), estimated the vmr of water vapor to be  $1 \times 10^{-6}$  at 2.5 bars increasing to  $\sim 3 \times 10^{-4}$  at 4 bars. Parallel studies by other authors found similar results (Drossart and Encrenaz 1982, Bjoraker *et al.* 1986, Lellouch *et al.* 1989). The mean vertical distribution obtained is a factor of 5 to 150 less than the “solar” value of  $1.5 \times 10^{-3}$ . Furthermore, to obtain good fits to their spectra, all of these models required some extra opacity in the 3.5 to 7 bar region, which was assumed to be evidence of a water cloud, since the temperature at which water vapor should condense falls within this range of pressure levels for all reasonable temperature profiles.

Later, an alternative view of the IRIS spectra was taken by Carlson *et al.* (1992, 1993), who showed that an acceptable fit to an average of the NEB hot spot spectra could be obtained by having a deep water vapor abundance of 1.5 solar condensing as a thick cloud at a pressure level of 4.9 bars, providing that the scattering properties of such a cloud were properly modelled instead of taken as a grey absorber. The relative humidity of water was inferred to be 100% at 4.9 bars, decreasing to 15% at 3 bars and then increasing again to 100% at 1 bar and remaining constant above. Later still, Roos-Serote *et al.* (1999) pointed out that the IRIS spectra include a slope in the continuum near  $5 \mu\text{m}$  which appears to be spurious, as it is not found in the later NIMS and ISO spectra. Correcting for this would remove the requirement for a deep water cloud in the hot spots to fit the IRIS data.

Two of the *Galileo* probe instruments provided information on the vertical profile of water vapor at the point of descent. As for the case with ammonia, the probe mass spectrometer water vapor data required empirical corrections to allow for the adsorption of water molecules in the inlet tube. It proved possible to infer an upper limit of  $6.9 \times 10^{-7}$  at pressures less than 3.8 bars, rising to  $(4.8 \pm 2.2) \times 10^{-5}$  at 11.7 bars and an order of magnitude larger  $(6.0 (+3.9/-2.8) \times 10^{-4})$  at 18.7 bars. The water vapor profile retrieved from the NFR measurements of Sromovsky *et al.* (1998) imply that the atmosphere in the region of probe

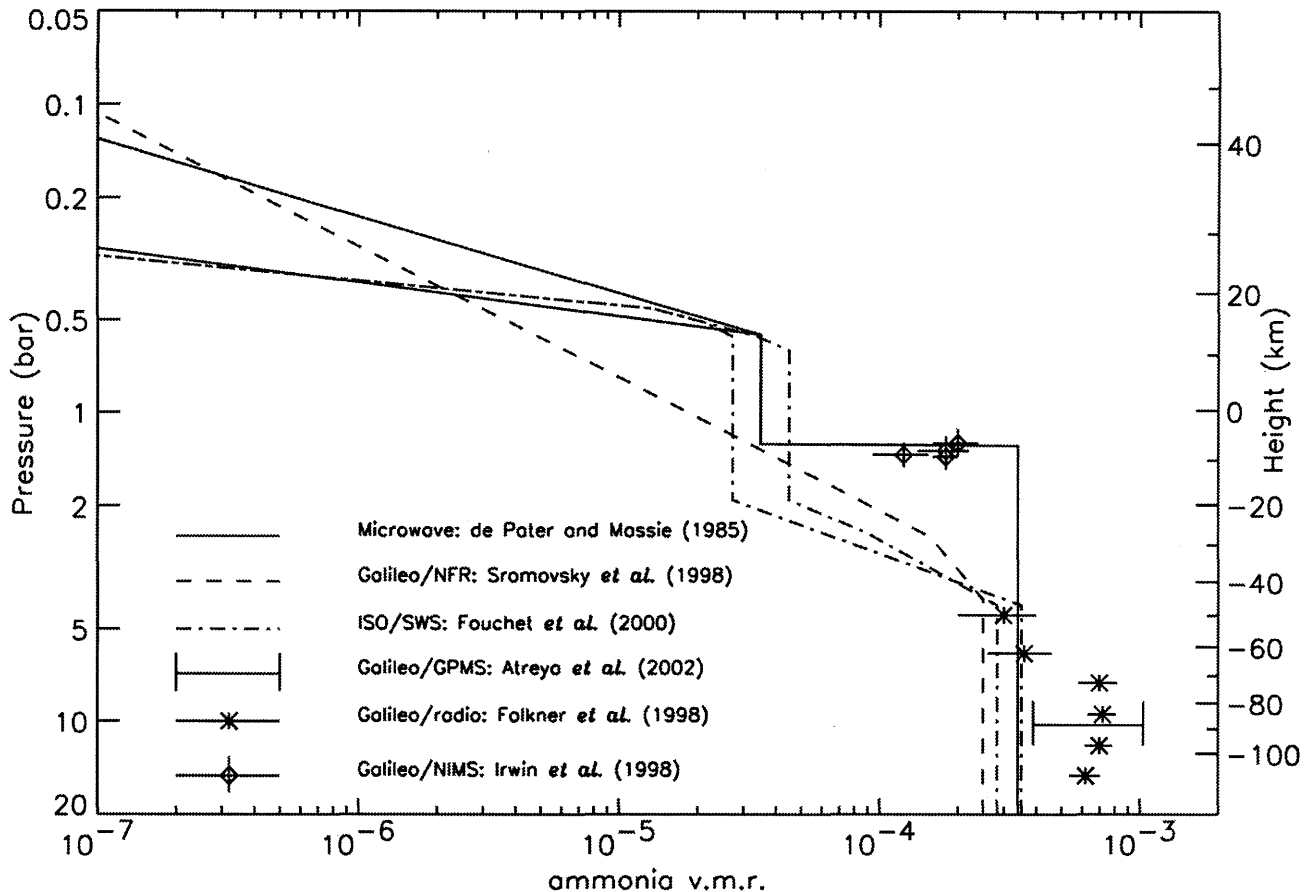


**Figure 4.4.** Models of the vertical profile of the ammonia volume mixing ratio, updated from Irwin (1999). The solid line, based on the analysis of microwave data by de Pater and Massie (1985), shows the effects of  $\text{NH}_4\text{SH}$  and  $\text{NH}_3$  cloud formation at about 1.4 and 0.5 bars respectively, and two limiting estimates of the effect of UV photolysis on the profile in the stratosphere. The dashed line, the cross-shaped points and the star symbols represent the profiles deduced from the *Galileo* Probe Net Flux Radiometer; four different *Galileo* NIMS spectra; and the *Galileo* probe uplink signal attenuation, respectively. The GPMS value of  $(7.1 \pm 3.2) \times 10^{-4}$  for the 8.6–12.0 bar region is shown by the horizontal bar. The dot-dashed lines represent  $\text{NH}_3$  profiles inside and outside a hot spot, as derived by Fouchet *et al.* (2000) from ISO-SWS observations.

descent is severely sub-saturated at pressures greater than approximately 1.5 bars.

All four IRIS and probe results are displayed in Figure 4.5, along with the vapor pressure curve for relative humidities of 10, 20, 50 and 100%, and the water vmr profiles corresponding to 0.1, 1 and 10 times the “solar” value. It can be seen that the two IRIS-based water vapor profiles, derived using different cloud models, are fairly consistent with each other, as are the two probe profiles derived from different instruments. However, there is a very marked difference between the mean probe and mean IRIS abundances, with the probe indicating much drier air at the heights where the data sets overlap. This difference is most likely attributable to real spatial and temporal variations in the humidity, as observed from orbit by NIMS. The implication is that the probe entered a region that was particularly dry even for a hot spot, while IRIS, with its fairly broad field-of-view, observed something closer to the average humidity in these  $5\mu\text{m}$ -bright regions.

Roos-Serote *et al.* (1998) and Irwin *et al.* (1998) inferred the water vapor amount in the 5–8 bar region from *Galileo* NIMS spectra. For regions with similar  $5\mu\text{m}$  brightness to that of the probe entry site, they both retrieved a mean rel-

ative humidity of around 10%. This value falls between the IRIS and probe profiles, and again suggests that the probe entry site was drier than the hot spot average. The maps of water vapor distribution derived from the NIMS data, (Roos-Serote *et al.* 2000) confirm that it does vary with position within a hot spot, and that in line with expectations relative humidity generally decreases as the  $5\mu\text{m}$  brightness increases, sometimes achieving values as low as 1%, consistent with the GPMS value. Elsewhere, it reaches values that correspond to near-solar oxygen abundances.

Turning now to the upper atmosphere, the ISO SWS and LWS instruments both detected water in the stratosphere at  $p \leq 10$  mb (Feuchtgruber *et al.* 1997, 1999, Lellouch *et al.* 2002), the latter at 66 and 99  $\mu\text{m}$ . The values from the two ISO instruments agree with each other, but are rather smaller than those inferred from the detection by the Submillimeter Wave Astronomical Satellite (SWAS) at 538  $\mu\text{m}$  (Bergin *et al.* 2000). This probably indicates that water is spatially and temporally variable at these high altitudes as well as in the troposphere.

The SWAS data further indicates that the mixing ratio of  $\text{H}_2\text{O}$  increases with height above about 10 mb. This is consistent with the expectation that the stratospheric water

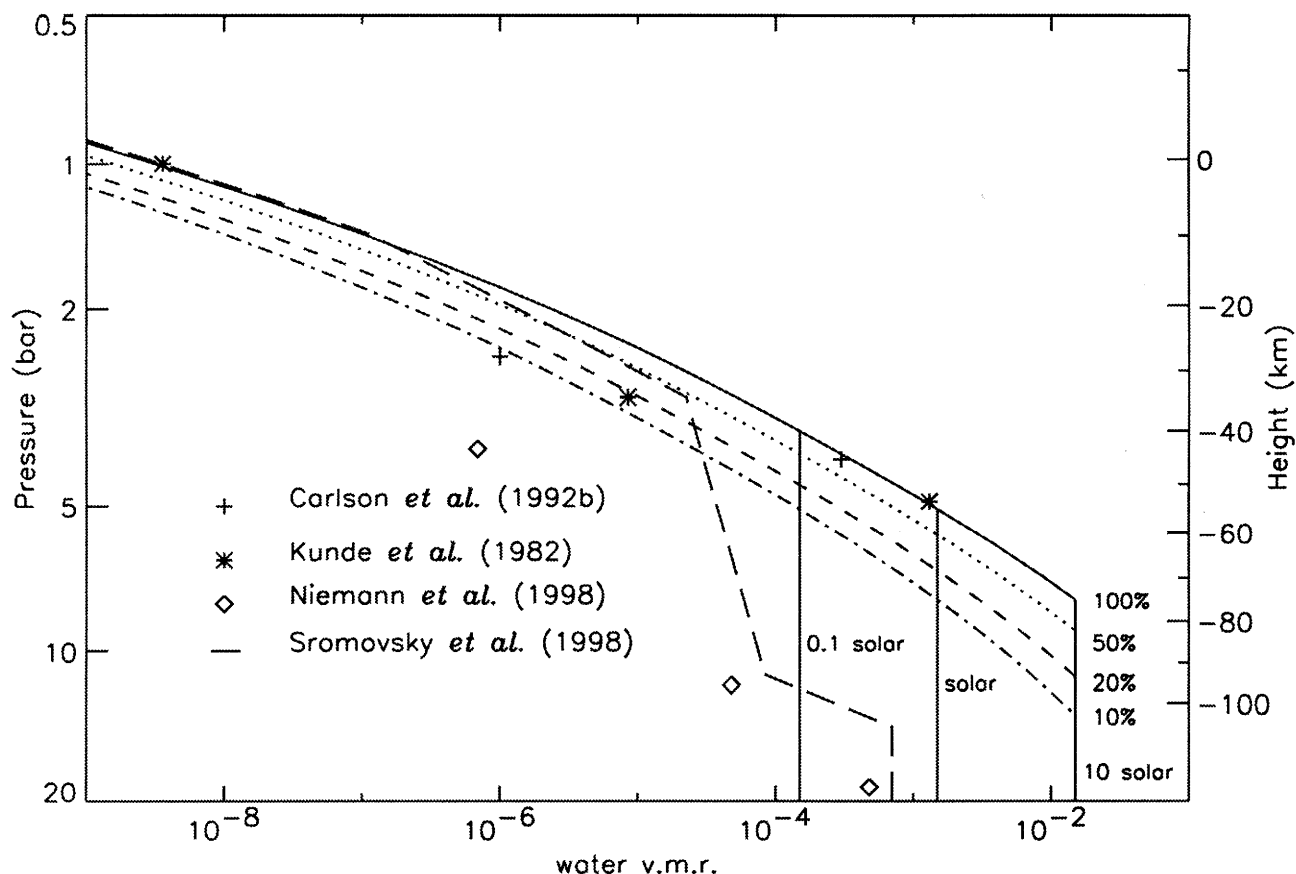


**Figure 4.5.** Models of the vertical profile of the water vapor volume mixing ratio, from Irwin (1999). The solid lines show deep vmrs of 0.1, 1, and 10 times the “solar” value of  $1.5 \times 10^{-3}$  below the saturation level, and the saturation vapor pressure curve above. The parallel curves are for 50, 20, and 10% relative humidity. The crosses and stars represent the best fit to the IRIS data by Carlson *et al.* (1992) and Kunde *et al.* (1982) respectively. The diamonds are from the GPMS by Niemann *et al.* (1998) and Atreya *et al.* (2002), and the dashed line is the best fit to the NFR data by Sromovsky *et al.* (1998).

vapor at high altitudes on Jupiter is mainly or entirely of external origin, arriving in the form of interplanetary dust and/or satellite or cometary material with a high ice content. The consequent fluctuations of the source in space and time, added to the effects of dynamics and photolysis, can be expected to produce a variable upper-atmospheric water distribution under normal conditions, as well as after extreme events like the SL-9 impact.

#### *Phosphine, Silane, Germane, and Arsine*

No significant information on phosphine ( $\text{PH}_3$ ) was obtained from the *Galileo* probe measurements. However, it has a very clear signature in the 5- $\mu\text{m}$  window and was detected prior to the *Voyager* encounter in ground-based spectra. Drossart *et al.* (1982), Kunde *et al.* (1982), and Bjoraker *et al.* (1986) determined mixing ratios from the IRIS spectra of  $5.2 \pm 1.7 \times 10^{-7}$ ,  $6.0 \pm 2.0 \times 10^{-7}$  and  $7.0 \pm 1.0 \times 10^{-7}$  respectively, while a recent analysis of the NIMS data by Irwin *et al.* (1998) gives a value of  $7.7 \pm 0.2 \times 10^{-7}$ . The error bars in the last value do not consider all sources of uncertainty and are therefore too small, so this set of numbers is reasonably consistent.

Above the 1 bar pressure level, UV radiation can dissociate phosphine, so its abundance there is reduced by an

amount that depends on the rate of vertical motion and on the overlying opacity. This behavior was first observed in a comparative study of the  $\text{PH}_3$  mixing ratios derived from different wavelengths, with the 5  $\mu\text{m}$  region probing the lower troposphere and the 8  $\mu\text{m}$  region the upper troposphere (Encrenaz *et al.* 1980). Carlson *et al.* (1993) found that a value of 0.3 for the ratio of the phosphine scale height to the total-pressure scale height fitted their measurements of thermal emission in the spectral region 900–1200  $\text{cm}^{-1}$ , in fair agreement with the theoretical predictions of Prinn and Lewis (1975) and Strobel (1977). This result was confirmed using NIMS data by Irwin *et al.* (1998), who obtained a scale height ratio of 0.27 by fitting to the spectrum between 4 and 4.5  $\mu\text{m}$ , which is dominated by reflected sunlight. The scale height ratio decreased with increasing 5  $\mu\text{m}$  brightness, as might be expected because the reduced cloud opacity in brighter regions allows deeper penetration of the solar UV radiation, and the brighter regions are characterized by more rapid downwelling.

Among the hydrides of elements less abundant than nitrogen and phosphorus that have been searched for spectroscopically are silane,  $\text{SiH}_4$ , germane,  $\text{GeH}_4$ , and arsine,  $\text{AsH}_3$ , and the last two have been found with volume mixing ratios of less than 1 ppb (Table 4.2). Silicon-containing gases are not expected in observable amounts even in rapid

updrafts because they condense as silicate clouds as deep as the 2000 K level. Germane is removed by conversion to the sulphide GeS and the selenide GeSe, but slowly enough that its observed abundance can be explained by vertical transport rates that are not unreasonable. A similar argument can be made concerning arsine, where the principal loss mechanism may be condensation of solid arsenic (Fegley and Lodders 1994).

#### Hydrocarbons

Higher hydrocarbons are produced from methane by photochemical processes in the upper atmosphere of Jupiter, augmented in the polar auroral regions by high-energy particle precipitation.

Ground-based observations provided the first detection of the most stable of these, ethane ( $C_2H_6$ ), along with acetylene ( $C_2H_2$ ) and its  $^{12}C^{13}CH_2$  isotope. *Voyager* IRIS added an upper limit for propane,  $C_3H_8$ , and detections of methylacetylene,  $C_3H_4$ , and benzene,  $C_6H_6$ , at high latitudes (Kim *et al.* 1985). Measurements by ISO (Fouchet *et al.* 2000) led to an upper limit for diacetylene,  $C_4H_2$ , while Bézard *et al.* (2001) reported the detection of ethylene,  $C_2H_4$ , and benzene at non-polar latitudes, from ground-based high-resolution spectroscopic measurements. The methyl radical,  $CH_3$ , previously detected in Saturn and Neptune by ISO, was finally found in Jupiter from CIRS spectroscopic observations at the time of the *Cassini* Jupiter flyby (Kunde *et al.* in preparation 2004).

These, and many other products which are predicted by models but have not yet been observed, diffuse or are transported by turbulence downwards through the stratosphere and into the troposphere, where they are eventually destroyed. Detailed theoretical accounts of the processes involved, model profiles and comparisons with measurements can be found in Chapter 7.

#### Carbon Monoxide and Dioxide

Shortly after the initial detection of CO in ground-based spectra (Beer 1975), it was found that this species has its highest mixing ratio above the tropopause, consistent with an external source (Beer and Taylor 1978b, Noll *et al.* 1997). It was debated for decades whether there is also a significant tropospheric abundance of this molecule, which would be contrary to the predictions of equilibrium chemistry models and imply therefore a source in the deep atmosphere and rapid vertical transport (Fegley and Lodders 1994).

Bézard *et al.* (2002b) observed hot spots on Jupiter in the 2080–2175  $cm^{-1}$  interval at the highest spectral resolution yet obtained (0.038  $cm^{-1}$ ), recording 12 lines of CO relatively free of other atmospheric absorption. They found the best fit to their spectra with constant mixing ratios of about  $0.75 \times 10^{-9}$  below the 200-mbar level and nearly an order of magnitude more,  $5 \times 10^{-9}$ , above. Although the vertical profile is likely to be more complex than this, it now seems clear that Jupiter has significant sources of CO both above and below the tropopause.

The ISO-SWS detected carbon dioxide emissions from the south polar and central regions of Jupiter, but not at the north pole, which suggests a possible origin in the impact of

Comet Shoemaker–Levy 9 at about 45°S in July 1994. A similar distribution of  $CO_2$  persisted until at least December 2000 when it was observed by the CIRS spectrometer on the *Cassini* spacecraft during its Jupiter encounter (Kunde *et al.* in preparation 2004).

#### Halogens and Halides

Jupiter undoubtedly contains the halogens fluorine, chlorine, bromine and iodine, but, except for a tentative detection of chlorine by the *Galileo* probe at pressures higher than 9 bars, none of these gases nor their compounds has been detected. This is not surprising, since the hydrogen halides HF, HCl, HBr and HI tend to combine rapidly with ammonia to form particles of solid ammonium salts. These will become part of the cloud system, leaving only miniscule amounts of the halide in the gaseous phase. Until the cloud and aerosol compositions have been measured much deeper in Jupiter's atmosphere than at present, it will not be possible to show how the halogen family of elements differs from a solar abundance. Table 4.3, from Showman (2001), shows values for the abundances expected in a solar model without chemical interaction with  $NH_3$  (Lodders and Fegley 1998) compared to the upper limits, where available, derived from spectroscopic attempts to observe the gaseous hydrogen halide.

#### Hydrogen Sulfide

Hydrogen sulfide is believed to be strongly depleted at and above the level where it reacts with  $NH_3$  to form  $NH_4SH$ , which condenses to form a cloud with its base near 2.2 bars (Atreya *et al.* 1999). This is probably why it has not been detected in remotely sensed spectra; the cloud is optically thick, and inhibits remote measurements of whatever  $H_2S$  may be present below the condensation level. Larson *et al.* (1984) set an upper limit of  $2 \times 10^{-8}$  for  $H_2S$  above the cloud, at the 0.7 bar level. The first actual detection was not until the *Galileo* probe mass spectrometer penetrated the atmosphere below the cloud, measuring a mixing ratio of  $7.7 \pm 0.5 \times 10^{-5}$  below the 16 bar level and  $7 \times 10^{-6}$  at 8.7 bars (Mahaffy *et al.* 2000). The GPMS also established an upper limit of about  $10^{-7}$  above 4 bars, consistent with the earlier limit from ground-based spectra. The deepest probe value is assumed to be representative of the interior of the planet; its significance for the S/H ratio in Jupiter is discussed below.

#### Chromophores in the Clouds

The question of what colors are present on Jupiter is made complicated by the fact that visual observations have a strong subjective component, while color photographs are difficult to calibrate (and, as often as not, are deliberately presented with the colors artificially “stretched”). In his overview in the first Jupiter book, Sill (1976) said “. . . it has been known for centuries that Jupiter has various shades of color: red (or pink, red-orange); brown (or red-brown and tan); blues (or blue-gray, purple-gray); grays; yellows (or yellow-brown, ochre, cream, greenish yellow); and perhaps even green.” Young (1985), on the other hand, did a photometric analysis and concluded that only various shades of

**Table 4.3.** Expected mole fractions for the halogen elements in Jupiter assuming solar abundances, compared to observed upper limits on gaseous HCl and HBr (from Showman 2001).

Element	Solar Mole Fraction	Observed Mole Fraction, 0–1 bar
F	$5 \times 10^{-8}$	-
Cl	$3 \times 10^{-7}$	$<5 \times 10^{-9}$ (Weisstein and Serabyn 1996)
Br	$7 \times 10^{-10}$	$<3 \times 10^{-9}$ (Noll 1996)
I	$6 \times 10^{-11}$	-

yellow are present. Both schools of thought still exist, but a modern consensus would probably admit white, yellows and browns, plus the brick-red tint of the Great Red Spot, as colors present on Jupiter with implications for the composition. The blues and greens, in particular, may be put down to optical effects rather than chromophores, but the GRS does seem to contain reddish material, as evidenced by the *Galileo* orbiter images which show the feature as much darker than its surroundings in the “blue” filter, while it is nearly neutral in brightness in the “red” filter (Dyudina *et al.* 2001). This conclusion has been supported by an analysis of HST images by Simon-Miller *et al.* (2001).

Some of the high, white clouds in the upper troposphere have been identified spectroscopically as ammonia ice crystals (Baines *et al.* 2002), and water ice features have been found in the *Voyager* IRIS spectra (Simon-Miller *et al.* 2000). The yellowish cast that covers most of the disk of Jupiter (and is a deeper yellow on Saturn) is probably due in part to photochemically-produced hydrocarbon droplets in the stratosphere, while the additional yellow and brownish hues in the clouds lying below the ammonia layer could conceivably be due to the presence of small amounts of the various allotropes of elemental sulfur, as noted by Prinn and Owen (1976). Ammonium hydrosulfide, thought to be the main constituent of this cloud, is white when pure, but it could be partially decomposed by the action of sunlight, releasing sulfur. Similarly, the reddish color of the GRS might be produced by elemental phosphorus, particularly if the material in the clouds forming this feature are relatively rich in phosphine or other compounds of that element, perhaps as a result of having been raised from a greater depth inside this giant vortex (Prinn and Owen 1976). A suggestion of phosphine enhancement in the GRS has been obtained very recently from spectral measurements by the CIRS instrument on *Cassini* (Kunde *et al.* 2004). However, West *et al.* (1986) did not find a good match in detail when they compared spectra of the GRS and a sample of red phosphorus.

In addition to these relatively simple possibilities, it is possible to speculate about an almost infinite range of other, progressively more complicated species which may be present in small amounts, dissolved in the principal cloud materials and contributing to the coloration. A mixture of simple and complex chemicals, conceivably including organics and polymers, may be responsible. The chemical nature of these “chromophores” is quite unknown, and likely to remain so for a considerable time to come, perhaps until an in situ analysis of the cloud materials is accomplished. Meanwhile, the detailed discussions of the various possibilities by Prinn and Owen (1976) and Sill (1976) remain relevant.

**Table 4.4.** Composition measurements in Jupiter’s atmosphere by the *Galileo* probe, *Voyager* and ground-based observatories, after Atreya *et al.* (2002) and references therein. The estimated errors in these values are typically about 20%; for a discussion of the uncertainties and more precise error estimates, see the original papers. For the special cases of He/H, D/H and  $^3\text{He}/^4\text{He}$ , see below. The solar elemental abundances used are from Anders and Grevesse (1989).

	Jupiter	Jupiter/Sun
<i>Elemental Ratio</i>		
Ne/H	$1.23 \times 10^{-05}$	0.1
Ar/H	$9.05 \times 10^{-06}$	2.5
Kr/H	$4.35 \times 10^{-09}$	2.7
Xe/H	$4.37 \times 10^{-10}$	2.6
C/H	$1.05 \times 10^{-03}$	2.9
N/H	$4.03 \times 10^{-04}$	3.6
O/H	$2.98 \times 10^{-04}$	0.35
P/H	$3.06 \times 10^{-07}$	0.82
S/H	$4.05 \times 10^{-05}$	2.5
<i>Isotopic Ratio</i>		
$^{13}\text{C}/^{12}\text{C}$	0.0108	0.10
$^{15}\text{N}/^{14}\text{N}$	0.0023	0.82
$^{36}\text{Ar}/^{38}\text{Ar}$	5.6	0.97
$^{136}\text{Xe}/\text{Xe}$	0.076	0.96
$^{134}\text{Xe}/\text{Xe}$	0.0091	0.09
$^{132}\text{Xe}/\text{Xe}$	0.29	1.09
$^{131}\text{Xe}/\text{Xe}$	0.203	0.94
$^{130}\text{Xe}/\text{Xe}$	0.038	0.87
$^{129}\text{Xe}/\text{Xe}$	0.285	1.04
$^{128}\text{Xe}/\text{Xe}$	0.018	0.82
$^{20}\text{Ne}/^{22}\text{Ne}$	13	0.94

### 4.3.2 Elemental and Isotopic Abundance Ratios

In this section we consider in more detail the relative abundances of constituents in Jupiter’s atmosphere, and the information that these convey about the origin and constitution of the planet and the solar system. Of particular interest are the ratios of the abundances of particular elements to hydrogen, of their isotopes to each other, and how Jupiter compares to the Sun in each case. Current values are summarized in Table 4.4.

#### *He/H*

Experimental determinations of the ratio of helium to molecular hydrogen in Jupiter’s atmosphere have converged on a value of 0.157, equivalent to a mole fraction of 0.136 (see Table 4.5) and a mass fraction of  $0.238 \pm 0.005$  (Table 4.6). This is almost exactly the same as the current best estimate for the proportion of helium in the Sun (Table 4.6).

It is tempting to believe that since (i) the planet and the star shared a common origin in the protosolar nebula, (ii) both are massive enough to have retained the same admixture of the light elements since their formation, and (iii) helium is chemically inactive, it should follow that they are expected to have the same hydrogen to helium ratio. Not only is that observed to be the case, but they are both equal to the current best estimates of the primordial value, obtained from studies of He/H in the extragalactic medium, in regions remote from star formation (essential since stellar interiors are a source of helium).

There are problems with this neat interpretation, unfortunately. Firstly, the protosolar value of He/H cannot be primordial because the Sun and planets contain heavy elements and therefore, by implication, additional helium made by earlier generations of stars. It follows that the protosolar cloud contained material from dead stars, in contrast to the extragalactic regions used to determine the primordial value. The latter show very small abundances of carbon, nitrogen, oxygen and other synthesised elements and hence do appear to consist primarily of material which has never been processed through stars. It must therefore be coincidental that the measured He/H ratio in Jupiter and the Sun is the same as the primordial number.

Such a coincidence is possible because the jovian and solar values apply only to the observable, outermost part of the atmosphere, and are not necessarily representative of the entire body in each case. In order to make a reliable comparison, it is necessary to understand the history of helium in both objects, taking this factor into account.

Theoretical studies suggest that condensation processes in the deep interior of Jupiter and Saturn concentrate helium there, to different degrees depending on their size and evolutionary history (see Chapter 3). It is expected that Uranus and Neptune will exhibit protosolar values of He/H as these planets do not contain liquid metallic hydrogen in which He can condense. The currently available measurements, summarized in Table 4.6, do show that the four giant planets have differing hydrogen to helium ratios, although not markedly so, particularly since the recent update to the value for Saturn by Conrath and Gautier (2000).

Current models of solar structure also suggest that the observed H/He ratio in the Sun is itself probably biased by a diffusive separation process that transfers helium towards the interior. In addition, the total amount of helium in the core of the Sun will have evolved from the protosolar value, as a result of fusion processes that convert hydrogen into helium. The best estimate of the solar modelers at the present time is that a net depletion of helium has taken place in the convective zone to which the measured H/He ratio applies. Working back to the protosolar helium abundance involves the use of evolutionary models that are constrained to fit the present age, radius and luminosity of the Sun (e.g., Bahcall and Ulrich 1988). Therefore the apparent agreement between the presently accepted values for the current ratio of helium to hydrogen in the Sun and in Jupiter appears to be just another remarkable coincidence.

#### D/H

Deuterium is not produced in significant quantities by any modern cosmic process, so the deuterium observed in

Jupiter, like all the rest, is primordial. It is, however, destroyed in stars by conversion to  $^3\text{He}$ , and so is not present in the Sun. The ratio of D/H in Jupiter might therefore be expected to provide the best estimate available to us of the protosolar value of this important ratio. A problem could arise, however, if Jupiter is highly enriched in primordial water ice, since the value of D/H in the ice is expected to be  $\geq 2$  times higher than that in  $\text{H}_2$  (Meier and Owen 1999). The proportion of ice that was incorporated into Jupiter during formation is unknown at present, in the absence of a reliable value for the global O/H ratio (see Table 4.7).

The earliest values for the D/H ratio in Jupiter were obtained from the ratio  $[\text{CH}_3\text{D}]/[\text{CH}_4]$ , together with a temperature-dependent fractionation factor to allow for the partitioning of deuterium between  $\text{CH}_3\text{D}$  and HD (Beer and Taylor 1973, 1978a). However, this approach is limited by the uncertainty in the partitioning of deuterium among the various hydrogen-containing molecules, and a more reliable value can be obtained directly from the ratio  $[\text{HD}]/2[\text{H}_2]$ . Early analyses of this kind used the HD lines in the visible to near-infrared range, which suffered from uncertainties due to difficulties in modeling the effects of multiple scattering on the atmospheric path lengths. This problem is much less serious when observations of the rotational lines in the far-infrared are considered. The intensity for the  $37.7 \mu\text{m}$  HD rotational line obtained by the Short Wave Spectrometer on the Earth-orbiting Infrared Space Observatory corresponds to  $\text{D}/\text{H} = 2.2 \times 10^{-5}$  (Encrenaz *et al.* 1996, Lellouch *et al.* 2001). This value is in good agreement with the same quantity derived from the mass spectrometers on the *Galileo* probe, viz.,  $(2.6 \pm 0.7) \times 10^{-5}$  (Table 4.7).

The table also shows the best current values for D/H in the other giant planets, the solar wind, meteorites, and the local interstellar medium. These are consistent with current models of the formation of the giant planets, in which the D/H ratio observed in the atmospheres of Jupiter and Saturn should equal the protosolar value, while in Uranus and Neptune, D/H is expected to be enriched due to low-temperature deuterium fractionation in the processes which formed their initial icy cores (Hubbard and McFarlane 1980, Lecluse *et al.* 1996). In the case of Jupiter, the initial core accounts for only 3% of the total mass of the planet, while it is more than 50% in the case of Uranus and Neptune.

The difference between the D/H ratio in Jupiter and that in the local interstellar medium suggests that some of the deuterium in the Sun's locality has been destroyed in the last 4.6 Gyr (noting with caution that the current local ISM is not the region in which Jupiter formed). The "primordial" value in the table was obtained from first generation, low-metallicity stars found in galaxies with high redshift, which are expected to retain their original, primordial deuterium, undiluted by the deuterium-depleted debris of any significant stellar evolution. This in turn suggests that the material making up the protosolar cloud had itself been depleted of about a third of its deuterium before it condensed to form the solar system.

#### $^3\text{He}/^4\text{He}$

A very small fraction, about 0.01%, of the helium in Jupiter is the isotope  $^3\text{He}$  ( $^3\text{He}/^4\text{He} = 1.66 \pm 0.05 \times 10^{-4}$ , Mahaffy *et al.* 1998). The proportion in the Sun, or at least in the

**Table 4.5.** Various estimates of the mole fraction (volume mixing ratio) of helium in Jupiter by successive space missions. The two *Voyager* values refer to preliminary and final analyses of the same IRIS data; the two *Galileo* values refer to measurements by two different probe instruments, the mass spectrometer and the Helium Abundance Detector. After von Zahn *et al.* (1998).

Mission	Mole fraction (= volume mixing ratio) of He	Reference
<i>Pioneer 10/11</i>	$0.12 \pm 0.06$	Orton and Ingersoll 1976
<i>Voyager 1</i>	$0.120 \pm 0.036$	Gautier <i>et al.</i> 1981
<i>Voyager 1</i>	$0.101 \pm 0.026$	Conrath <i>et al.</i> 1984
<i>Galileo</i> (GPMS)	$0.136 \pm 0.026$	Niemann <i>et al.</i> 1998
<i>Galileo</i> (HAD)	$0.1359 \pm 0.0027$	von Zahn <i>et al.</i> 1998

**Table 4.6.** Helium mass fractions in Jupiter; the other giant planets; the outer part of the present Sun; the protosolar nebula; and the intergalactic medium (primordial). Updated after von Zahn *et al.* (1998).

	Helium Mass Fraction	Reference
Jupiter ( <i>Galileo</i> HAD)	$0.238 \pm 0.005$	von Zahn <i>et al.</i> 1998
Jupiter ( <i>Voyager</i> )	$0.18 \pm 0.04$	Conrath <i>et al.</i> 1984
Saturn ( <i>Voyager</i> )	$0.21 \pm 0.03$	Conrath and Gautier 2000
Uranus ( <i>Voyager</i> )	$0.262 \pm 0.048$	Conrath <i>et al.</i> 1987
Neptune ( <i>Voyager</i> )	$0.32 \pm 0.05$	Conrath <i>et al.</i> 1981
Sun	$0.24 \pm 0.01$	Basu and Antia 1995
Protosolar	$0.275 \pm 0.01$	Bahcall and Ulrich 1988
Primordial	$0.232 \pm 0.005$	Olive and Steigmann 1995

solar wind where it can be measured, is larger ( $4.4 \pm 0.4 \times 10^{-4}$ , Bodmer *et al.* 1995), owing to the fact that the deuterium destroyed in the Sun was converted to  $^3\text{He}$ , augmenting the protosolar value of  $^3\text{He}/^4\text{He}$ .

If the  $^3\text{He}/^4\text{He}$  ratio in Jupiter is indeed protosolar, then subtracting this from the present-day solar value gives an estimate of the fractional abundance of  $^3\text{He}$  that was produced from the deuterium that was originally present in the Sun, which in turn gives an estimate of the protosolar D/ $^4\text{He}$  ratio. If the resulting value for the protosolar value of D/He, i.e.,

$$[(4.4 \pm 0.4) - (1.66 \pm 0.05)] \times 10^{-4} = (2.7 \pm 0.3) \times 10^{-4} \quad (4.1)$$

is multiplied by the protosolar value of He/H of 0.1 as adopted by Mahaffy *et al.* (1998), the inferred protosolar D/H is  $2.7 \pm 0.3 \times 10^{-4}$ . This is in excellent agreement with the GPMS measurement of the D/H ratio in present-day Jupiter, which is  $2.6 \pm 0.7 \times 10^{-5}$  (see previous section). This agreement supports the theoretical expectation that D/H as well as  $^3\text{He}/^4\text{He}$  has the protosolar value in Jupiter.

#### C, P, N, S, O

The value from *Voyager* spectroscopy for the ratio of  $\text{CH}_4$  to  $\text{H}_2$  was  $2.2 \times 10^{-3}$  (Gautier and Owen 1989), in good agreement with the *Galileo* probe ( $2.1 \pm 0.4 \times 10^{-3}$ ; Niemann *et al.* 1998). The corresponding C/H abundance ratio is 2.9 times the solar value, and the significance of this ratio is further discussed below.

The ratio of  $^{13}\text{C}/^{12}\text{C}$  found by the *Galileo* probe ( $0.0108 \pm 0.0005$ , Niemann *et al.* 1998, Atreya *et al.* 2002) confirms with smaller error bars the ground-based value found from spectroscopic measurements of methane (Combes *et al.* 1977) and ethane (Sada *et al.* 1996). These values are close to terrestrial and suggest a protosolar value

with little or no fractionation of carbon isotopes in the atmosphere of Jupiter and the other outer planets.

The P/H ratio is more difficult to establish than C/H, because  $\text{PH}_3$  is depleted in the upper troposphere and above by photodissociation and in the deeper atmosphere it should be oxidized by  $\text{H}_2\text{O}$  to form  $\text{P}_4\text{O}_6$ . The fact that it nevertheless has been detected was explained by Prinn and Owen (1976) in terms of rapid vertical mixing that transports  $\text{PH}_3$  to the upper atmosphere from depths where the temperature exceeds 800 K and the molecule is expected to be stable.

The  $\text{PH}_3$  mixing ratio measured in the deep troposphere corresponds quite closely to the solar P/H ratio (Table 4.4). This again could be coincidental, since the  $\text{PH}_3$  mixing ratio is primarily a diagnostic of vertical mixing, as exemplified by the behavior of Saturn, where it is considerably higher. *Voyager* found a P/H enrichment by a factor of about 3 over the solar value on Saturn (Gautier and Owen 1989) while ground-based observers (Noll and Larson 1991, Orton *et al.* 2001) have reported higher values, suggesting variability.

$\text{NH}_3$  is also strongly depleted in the upper troposphere, in this case by condensation to form clouds as well as by photolysis. The  $\text{NH}_3$  mixing ratio in the deep atmosphere has been inferred from the inversion band centered at 1.35 cm in the jovian radio spectrum, which indicates a possible N/H enrichment by a factor of two over solar, with a similar factor on Saturn (de Pater and Massie 1985). Additional information about the deep  $\text{NH}_3$  mixing ratio provided by the radio signal of the *Galileo* probe (Section 4.3) indicated an N/H enrichment by a factor of about four at pressures higher than 7 bars (Folkner *et al.* 1998).

Owen *et al.* (2001) derived a value of  $^{15}\text{N}/^{14}\text{N} = 2.3 \pm 0.3 \times 10^{-3}$  in the jovian atmosphere using data from the *Galileo* Probe Mass Spectrometer, in agreement with the value of  $^{15}\text{N}/^{14}\text{N} = 1.9 (+0.9/-1.0) \times 10^{-3}$  found at 400 mbar from a study of  $\text{NH}_3$  absorptions in the ISO spectra

**Table 4.7.** Deuterium to hydrogen ratios in various bodies. Updated from Encrenaz (1999).

Object	D/H	Reference
Jupiter ( <i>Galileo</i> )	$2.6 \pm 0.7 \times 10^{-5}$	Mahaffy <i>et al.</i> 1998
Jupiter (ISO, from HD)	$2.4 \pm 0.4 \times 10^{-5}$	Lellouch <i>et al.</i> 2001
Saturn (ISO)	$1.7 (+0.7/-0.4) \times 10^{-5}$	Lellouch <i>et al.</i> 2001
Uranus (ISO)	$5.5 (+3.5/-1.5) \times 10^{-5}$	Feuchtgruber <i>et al.</i> 1999
Neptune (ISO)	$6.5 (+2.5/-1.5) \times 10^{-5}$	Feuchtgruber <i>et al.</i> 1999
Protosolar (from solar wind $^3\text{He}$ $^4\text{He}$ )	$2.1 \pm 0.5 \times 10^{-5}$	Geiss and Gloeckler 1988
Meteoritic and Lunar	$2.6 \pm 1.2 \times 10^{-5}$	Geiss 1993
Local Interstellar Medium	$1.6 \pm 0.12 \times 10^{-5}$	Linsky 1996
Primordial	$3.4 \pm 0.25 \times 10^{-5}$	Burles and Tytler 1998

of Jupiter (Fouchet *et al.* 2000). Owen *et al.* (2001) argue that this is likely to be the protosolar value, and that the nitrogen in Jupiter (and the Sun) was probably delivered primarily as  $\text{N}_2$ , rather than as compounds of nitrogen such as ammonia or hydrogen cyanide.

Hydrogen sulfide remains undetected by spectroscopy, probably because it is strongly depleted by reaction with  $\text{NH}_3$  to form the  $\text{NH}_4\text{SH}$  cloud layer based at about 2.2 bars (Section 4.9). However, the GPMS measured an enrichment of S/H by a factor of 2.5, relative to solar, in the deep atmosphere at pressures higher than 16 bars.

The discussion above about the principal oxygen-bearing species,  $\text{H}_2\text{O}$ , described how the available data is biased towards the relatively dry hot spot regions. The inferred upper tropospheric abundances, typically in the range of a few parts per million at pressures of 2 to 4 bars, are not therefore typical of the whole planet, although they would imply very strong depletion of O/H with regard to the solar value if they were. The *Galileo* probe confirmed the low values for the humidity in a hot spot at the levels probed by the 5  $\mu\text{m}$  spectra, but found that the O/H ratio lower down increased with pressure to reach about 0.35 times solar at a pressure of 18.7 bars (Niemann *et al.* 1998). At this point the mixing ratio of  $\text{H}_2\text{O}$  was still increasing, so apparently the probe did not survive to the depths in the jovian troposphere below the local  $\text{H}_2\text{O}$  condensation level where the value of O/H inferred from the  $\text{H}_2\text{O}$  mixing ratio would be representative of its value in Jupiter as a whole. Hence the last probe measurement is a lower limit, and the global value of O/H must still be considered undetermined.

#### Noble Gases

Noble gases other than helium were identified for the first time in Jupiter by the GPMS instrument on the *Galileo* probe (Niemann *et al.* 1998, Atreya *et al.* 2002). In Jupiter, Ne is strongly depleted with respect to its solar value, with an Ne/H ratio equal to 0.13 times the solar value or less. The Ar/H, Kr/H and Xe/H jovian ratios, however, are enhanced to 2.5, 2.7, and 2.6 times the solar value, respectively. As suggested by Stevenson and Salpeter (1976), the low Ne abundance is probably caused by a fractionation effect related to that which transfers helium from the outer to the inner regions of Jupiter (Section 5.1). Helium is predicted to form droplets at high pressures that “rain out” of the deep atmosphere towards the center of the planet under the

effects of gravity. Neon is soluble in the helium drops and apparently suffers the same fate as a result.

Isotopic ratios in Ne, Ar, Kr and Xe in Jupiter were all found to have the solar wind values within experimental error (Niemann *et al.* 1998, Mahaffy *et al.* 2000, Atreya *et al.* 2002).

#### 4.3.3 Processes Affecting Composition and its Variability

##### Condensation and Cloud Formation

In the pressure range from 10 bars to the top of the atmosphere, the existence of at least four different types of condensate cloud has been tentatively established. The chemical properties of condensed, as opposed to gaseous, material are difficult to measure spectroscopically or in situ with a probe, so the evidence for the properties of these layers remains predominantly indirect. Nevertheless, a fairly consistent picture, albeit with many important gaps, has gradually emerged.

The deepest of the cloud layers, consisting principally of  $\text{H}_2\text{O}$ , is expected from thermophysical models (Weidenschilling and Lewis 1973, Atreya *et al.* 1999) to form in the region near 5 bars, where the temperature is around 273 K. Above that, near 2.2 bars and 210 K, the same models predict  $\text{H}_2\text{S}$  condensation, probably as ammonium compounds, and most likely predominantly  $\text{NH}_4\text{SH}$ . Sufficient ammonia remains to form a cloud layer of  $\text{NH}_3$  ice crystals between about 0.7 bars and the tropopause. Higher, in the upper stratosphere and lower thermosphere, lies a thin haze of hydrocarbon droplets, formed by the photochemical action of sunlight on the methane and other molecules in Jupiter’s atmosphere. Methane itself never gets cold enough to condense on Jupiter, unlike the case on Uranus and Neptune. All of these clouds show complex behavior in space and time, as is described in Chapter 5.

##### Photochemistry

The gaseous composition of the atmosphere in the cloud-forming region is affected by photochemical as well as condensation processes. For instance, as already noted, the depletion of ammonia above the 2 bar level and below its condensation level is unlikely to be due entirely, or even principally, to the formation of the  $\text{NH}_4\text{SH}$  clouds, because this would require 10 times the solar abundance of sulfur rather

than the factor of three actually observed in Jupiter. Photolytic destruction involving UV radiation at wavelengths between 160 and 235 nm is the most likely process accounting for the rest of the “missing” ammonia.

Most of the ultraviolet solar radiation falling on Jupiter is deposited in the stratosphere, where the most intense photochemical activity, primarily involving methane, occurs. The solar penetration level is fixed at each wavelength by Rayleigh scattering and determines, for each molecule, the altitude range over which photodissociation takes place. In Jupiter, the solar flux between 60 and 80 nm is absorbed by H<sub>2</sub>, at very high atmospheric levels ( $P \sim 10^{-9}$  bar) it is absorbed at about 1  $\mu$ bar by CH<sub>4</sub> between 90 and 115 nm, and around 0.1 mb between 140 and 170 nm by hydrocarbons. Significant photodissociation of NH<sub>3</sub> and PH<sub>3</sub> takes place at lower levels, peaking at the 80 mbar level for PH<sub>3</sub>, and around the tropopause (30–300 mb) for NH<sub>3</sub> (Atreya 1986). The tail of the photolysis curve for ammonia extends down to the NH<sub>4</sub>SH cloud condensation level near 2 bars, and, as we have seen, appears to affect the abundance at and somewhat below the cloud level in situations that involve large-scale downwelling motions.

The main products of ammonia photolysis are hydrazine (N<sub>2</sub>H<sub>4</sub>) and N<sub>2</sub> (Atreya *et al.* 1999). N<sub>2</sub>H<sub>4</sub> is expected to condense, which explains its non-detection as a gaseous species in the jovian infrared spectrum, although it and other products may contribute to the upper tropospheric haze. According to Atreya and Romani (1985), the expected mixing ratio of N<sub>2</sub> is between  $10^{-11}$  and  $10^{-9}$ , but the species could not be measured by the GPMS because mass number 28 is also occupied by CO and C<sub>2</sub>H<sub>4</sub>.

Phosphine is some three orders of magnitude less abundant in the photochemical region of the atmosphere than ammonia and, as already noted, the fact that it is present at all probably implies rapid vertical transport from the deep atmosphere. The final product of PH<sub>3</sub> photodissociation is triclinic red phosphorus, P<sub>4</sub> (Prinn and Lewis 1975, Atreya, 1986), which may contribute to the coloration of the clouds. In particular, since the GRS is a region of particularly strong vertical mixing (probably from greater depths and certainly to higher levels in the atmosphere than elsewhere on the planet), its reddish color might be due to a relatively high concentration of these crystals. Spectroscopic identification is more difficult for solids than for gases, however, and experimental confirmation is still lacking.

The photochemistry of methane is complex and involves a large number of reactions. The major stable products, formed in the 10 mbar to 1  $\mu$ bar region, are C<sub>2</sub>H<sub>2</sub>, C<sub>2</sub>H<sub>6</sub> and C<sub>2</sub>H<sub>4</sub>, with CH<sub>3</sub> as an unstable intermediate species. C<sub>2</sub>H<sub>2</sub> may form polyacetylenes by catalytic conversion. The C<sub>3</sub> hydrocarbons expected to be most abundant are C<sub>3</sub>H<sub>8</sub> (propane) and C<sub>3</sub>H<sub>4</sub> (methylacetylene), with mixing ratios peaking as high as  $10^{-6}$  at maximum production level (1 mbar to 1  $\mu$ bar), and smaller amounts of C<sub>4</sub>H<sub>10</sub> and C<sub>6</sub>H<sub>6</sub>.

The oxygen-bearing molecules H<sub>2</sub>O, CO and CO<sub>2</sub> that have been detected in the stratosphere of Jupiter are thought to be at least primarily of external origin. It is unclear at present how much of the CO<sub>2</sub> and CO is present as ices in the infalling material, and how much is formed chemically in the atmosphere, after the delivery of the necessary oxygen in the form of water, by reactions in which the carbon is supplied by methane and its photochemical products.

Numerical models have been used extensively to evaluate the principal photochemical cycles and predict the abundances of the expected dissociation products in detail. The observations used to test these are augmented at low atmospheric pressures by information from stellar occultations observed in the ultraviolet spectral range. For details see Chapter 7.

### *Deep Atmospheric Chemistry*

Most of the atmosphere of Jupiter lies below the maximum pressure of direct observations by spectroscopy or the *Galileo* probe (about 20 bars) but processes at depth have an important effect on the composition of the outer, observable part of the atmosphere through vertical mixing in both directions. The species thought to be most affected by downward transportation are helium and neon, which form droplets at the  $\sim 1$  Mbar level that then “rain out” further towards the core (see below and Chapter 3). Other species, most notably CO, PH<sub>3</sub>, GeH<sub>4</sub>, and AsH<sub>3</sub>, travel in the opposite direction and are present in the upper troposphere only as a result of rapid upward convection from deeper levels where the temperature is high enough so that the reactions that form them can proceed.

Apart from inferences that can be made from the observed abundances of these species, our knowledge of the composition and chemistry of the deep atmosphere depends entirely on models, the most comprehensive of which is that of Fegley and Lodders (1994). This considers all of the stable elements in the periodic table in their observed abundances, with a common enrichment factor of 2.3 (based on the then-current value for C as derived from CH<sub>4</sub>), relative to solar, for those elements for which no experimental value has been obtained. Reactions involving more than 2000 compounds are then computed and the resulting abundances plotted along a jovian adiabatic temperature-pressure profile, extrapolated downwards from the measured profile near the top of the troposphere, taking condensation of solid and liquid products into account. The results and a discussion of the many uncertainties, including the reaction paths and rate constants, are presented in detail in the original paper. By way of illustration, it can be noted that they predict the condensation of ammonium iodide, NH<sub>4</sub>I, at a temperature of 368 K, some 80 km below the more familiar ammonium hydrosulfide NH<sub>4</sub>SH clouds that form part of the visible face of the planet. After passing through this, and dozens of other cloud layers of exotic composition, some future deep-atmosphere probe may also encounter a thin cloud of metallic silver near the 1000 K temperature level.

### *Dynamics and Vertical Transport*

The existence of deep convection on Jupiter, with the effects on the atmospheric composition already discussed, is well accepted, but details such as the vertical extent of individual cells, the role of waves and of eddy mixing, and their variations in latitude and longitude over the globe are poorly known (see Chapter 6 by Ingersoll *et al.*). The fact that the abundance of water vapor is still increasing at 20 bars, the level where the probe signal was lost, suggests that mixing is incomplete above this depth at least for this species at

that location. The probe Doppler wind experiment (Atkinson *et al.* 1998), which inferred horizontal winds from the Doppler shifting of the transmitted probe signal, observed zonal wind speeds of approximately  $90 \text{ m s}^{-1}$  at 0.5 bar, rising to  $170 \text{ m s}^{-1}$  by about 4 bars and remaining fairly uniform with increasing depth thereafter. The apparent absence of zonal wind shear between 4 and 20 bars suggests a consistent dynamical regime down to at least these levels. Presumably this includes the large-scale convection patterns marked by the belt–zone cloud structure. The implication is that, despite the high zonal winds, there is only limited horizontal mixing in the meridional direction between the rising and descending branches. The probe data further imply that this mixing is efficient enough to mix ammonia and the other species that are more volatile than  $\text{H}_2\text{O}$  and hence condense higher in the atmosphere, or not at all, above the 20 bar level on Jupiter.

As already noted, chemical models predict very low phosphine abundances in the visible part of the atmosphere, although it is the principal phosphorus compound at temperatures above about 500 K (Fegley and Lodders 1994). Its detection in the amounts described above (Section 4.5) is considered clear evidence for vertical transport on timescales faster than the chemical conversion rates. It follows that other non-equilibrium species may be observed, particularly those that convert to condensable products relatively slowly. It also follows that the observed abundances will be higher in upwelling regions of the atmosphere, but unfortunately that means in the zones, where observations are difficult because of the dense high cloud cover. The eddy diffusion coefficient can be obtained from the heat flux using mixing-length theory, and the value obtained is similar to that required by the presence of non-equilibrium molecules (Lunine and Hunten 1987).

In principle, mapping of readily observable non-equilibrium compounds such as phosphine across the jovian disk will provide information about the global variability of the efficiency of vertical convection. Some preliminary, and so far fairly inconclusive, work along these lines has been carried out using *Galileo* NIMS data (e.g., Irwin *et al.* 1998). Studies of the ratio between the ortho and para states of hydrogen, which is temperature dependent, also potentially yield information about the vertical convection rate and its variability. In equilibrium, the ortho–para ratio is 3:1 for temperatures above about 300 K, with the proportion of para increasing at lower temperatures. The rate of equilibrium is very slow, of the order of tens of years, in the laboratory, but on Jupiter it is essentially unknown since it may be much faster if it is catalysed, for example by collisions with radiation-damaged ammonia ice particles (Massie and Hunten 1982).

The jovian ortho–para ratio can be inferred from the far-infrared spectrum, which is dominated by the broad S(0) and S(1) pressure-induced pure rotational lines of hydrogen. The most recent analysis of the *Voyager* IRIS spectra for this purpose by Conrath *et al.* (1998) retrieved the para fraction in the pressure range from 0.08 to 0.5 bars, at latitudes from  $60^\circ\text{S}$  to  $60^\circ\text{N}$ . The results show higher para fractions at low latitudes, suggesting that the most rapid upwelling from the warmer depths occurs near the equator, although higher latitudes also exhibit slightly higher para abundances

than the equilibrium values at the relevant temperatures, indicating vigorous convection there as well.

#### *External Sources of Water and Other Species*

The detection of  $\text{H}_2\text{O}$  and  $\text{CO}_2$  in the upper atmosphere of Jupiter (Lellouch *et al.* 1997, 2002), along with CO, which had been detected much earlier by ground-based spectroscopy (Beer 1975), implies the existence of an external supply of oxygen. The observations of water vapor are compatible with a mean mixing ratio of about  $10^{-9}$  above the 15 mbar level, and an incoming flux of about  $10^6$  molecules  $\text{cm}^{-2} \text{ s}^{-1}$  (Lellouch *et al.* 1997). The source could be either an interplanetary (or even interstellar) flux of meteorites and comets, or a local source originating from the icy satellites and/or rings. For the time being it is difficult to determine which source is dominant, although the similarity in the inferred value of the incoming flux of  $\text{H}_2\text{O}$  on all of the outer planets, and Titan, would seem to favor the interplanetary source (Feuchtgruber *et al.* 1997).

A spectacular example of the arrival of material from space on Jupiter was provided by the impact of the Comet Shoemaker–Levy 9 in July 1994. The event was extensively studied by means of infrared ground-based observations and the *Galileo* NIMS spectrometer. The composition of Jupiter’s atmosphere was observed to change dramatically around the impact site as a result of the introduction of a huge mass of dust and volatiles, plus the chemistry resulting from the high temperatures during impact. From this extreme event, some limited inferences can be drawn about the effect on the composition of Jupiter’s atmosphere of the daily incursion of a much larger number of much smaller cometary and meteoritic objects. For a full discussion of the SL-9 impact, the observations made, and their interpretation, see Chapter 8 by Harrington *et al.* The following is a very brief summary.

The molecules reported as having been observed, either for the first time or with a large enhancement over the normal amounts, during the splash phase of SL-9 (and in some cases, for a considerable period afterwards) are: dust (silicates and possibly organics);  $\text{H}_2\text{O}$ ,  $\text{CO}_2$  and CO;  $\text{S}_2$ ,  $\text{CS}_2$ , CS, OCS, HCN,  $\text{C}_2\text{H}_4$ , and  $\text{NH}_3$ ; possibly  $\text{PH}_3$  and  $\text{H}_2\text{S}$ ; and certain metallic lines in the UV and visible range. It is not possible to say with certainty what was the origin of each of these. Along with the dust and metals, large amounts of  $\text{H}_2\text{O}$  and CO were undoubtedly present in the comet itself as ices that were vaporised during the impact. Other species known to be already present on Jupiter, although normally in much smaller amounts, like  $\text{NH}_3$ , may have been drawn up into the upper atmosphere from deep levels, where they are more plentiful, in the disturbance following the collision. The remainder may have been chemically produced in the fireball, where the temperature reached several thousands of degrees K for some tens of minutes, from a mixture of cometary and atmospheric molecules, including vaporised cloud materials.

For several species, it is possible that two or even all three of these sources may have been involved to a significant degree. Hydrogen cyanide, which may be the best example, was seen in the upper atmosphere in concentrations that are found, according to chemical equilibrium models, only at depths well below the sulfur-containing clouds. However,

it could also be chemically produced, from derivatives of ammonia and methane, and it is not unreasonable to assume that it was also present in the comet. Models that attempt to unravel the various processes at work and explain the data are presented in Chapter 8.

#### 4.3.4 Origin and Evolution of Jupiter's Atmosphere: Constraints Imposed by Compositional Measurements

Composition measurements in the deep troposphere, below the levels where condensation takes place, can be assumed with some caution to represent bulk values for Jupiter, except for the case of helium, which, as discussed above, "rains out" at depth, neon, which is soluble in the helium drops and suffers the same fate, and oxygen, which is present as water that is not well mixed until depths below those for which we have data. It remains then to explain the enrichment with respect to the solar value in carbon, sulfur, nitrogen and the noble gases by factors between two and four. As discussed in Section 2, these enrichments would not be present if Jupiter formed from a simple condensation of the solar nebula, so they imply a combined nucleation and collapse mechanism whereby a heavy nucleus initially accreted, achieving sufficient mass to attract additional planetesimals and gas.

If these planetesimals formed in the region of the giant planets, then they should be strongly depleted in neon, argon and nitrogen, because the temperatures were too high for these volatile gases to be trapped effectively in ice. However, Owen *et al.* (1999) found a value of  $2.5 \pm 0.5$  times the solar value for the argon mixing ratio, clearly indicating enrichment over the expected solar nebular value. They also found krypton and xenon to be similarly enhanced, at  $2.7 \pm 0.5$  and  $2.6 \pm 0.5$  times the solar values, respectively. Thus it appears that, contrary to expectations, these heavy noble gases share essentially the same enrichment on Jupiter as carbon, sulfur and nitrogen and probably everything else except neon and helium, for which special considerations apply (Fig. 4.6).

This requires that argon, krypton, xenon and nitrogen were present in solar proportions relative to carbon and sulfur in the icy planetesimals that contributed to Jupiter's formation. Laboratory studies of the trapping of highly volatile gases in amorphous ice forming at temperatures below 75 K by Owen and Bar-Nun (1995) have shown that trapping argon and  $N_2$  in solar abundances relative to carbon in icy planetesimals requires condensation of the ice at temperatures below 30 K (capturing neon in this proportion requires a temperature  $T < 17$  K).

Owen *et al.* (1999) proposed that the uniform enrichment of heavy elements that is observed on Jupiter must mean that these elements came to the planet in very cold ( $T < 30$  K) icy planetesimals. This differs from conventional models, which relate the formation of giant planets to the threshold distance from their stars where it first becomes cold enough for water ice to condense in the circumstellar disks. In these "snowline" models, the ice condenses at  $T = 150$  K ( $\sim 5$  AU in our solar system). Ar and  $N_2$  would be depleted by over four orders of magnitude in icy planetesimals formed at such high temperatures.

It remains to be shown how planetesimals that formed at the very low temperatures required to explain the ob-

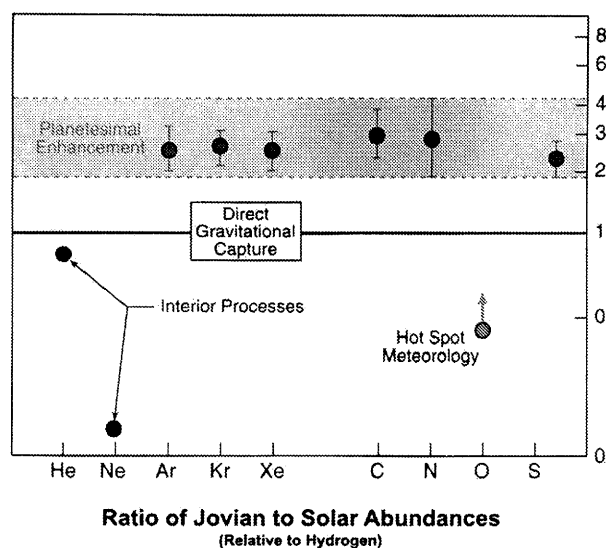


Figure 4.6. Elemental abundances (relative to hydrogen) in Jupiter's atmosphere, compared to solar abundances. Updated from Owen *et al.* 1999.

servations could have found their way to Jupiter. Did they form in the local interstellar medium prior to, or during, the collapse of the fragment that formed the original solar nebula? Or perhaps the solar nebula was in fact much colder than current models predict? A possible solution was proposed by Gautier *et al.* (2001a,b), in which the water in the proto-jovian planetesimals froze, not as amorphous ice, but in the crystalline form, trapping the volatile compounds of the heavy elements in the ice lattice as clathrates. However, argon clathrate is only stable at temperatures below 38 K, hence the requirement for remarkably low temperatures persists in this interpretation.

Gautier *et al.* further pointed out that the formation of clathrates requires much more water per trapped molecule than does trapping in amorphous ice. They predict that the O/H ratio in Jupiter will be significantly larger than the C/H ratio, at least nine times solar even if clathrate formation was 100% efficient. Unfortunately, this test cannot be applied at present since, as we have seen above, there is no measurement of the O/H ratio that can be taken as representative of Jupiter as a whole. However, there is a test that can be made in the case of sulfur, where the clathrate theory also predicts an excess of S/H compared with other elemental abundances. The fact that this was not observed by the GPMS at the level required by the clathrate theory is tentatively attributed by Gautier *et al.* (2001a) to the combination of sulfur with iron to form FeS in the inner solar nebula, a proposal that Atreya *et al.* (2002) find quantitatively unsupportable. The amount of sulfur that must be sequestered through this process in the inner nebula is 0.22 Earth masses ( $M_E$ ). The amount of sulfur in the Earth is  $0.02 M_E$ , Venus presumably has a similar endowment and the entire mass of Mars is only  $0.11 M_E$ . Hence some other explanation for the missing sulfur would seem to be required.

As Owen *et al.* (1999) note, the difficulties inherent in all of these suggestions serve to emphasize the significance of the constraint which composition measurements place on Jupiter's formation and history. A fuller discussion of the problem can be found in Chapter 2 by Lunine *et al.*

#### 4.4 SUMMARY AND CONCLUSIONS

The composition of Jupiter's observable atmosphere, i.e., that part down to a pressure of about 20 bars for which direct measurements exist, is now reasonably well understood in broad terms. The details of the interior processes that deplete helium and neon, the meteorological activity that raises non-equilibrium compounds from intermediate depths, the cloud chemistry, and the photochemical behavior at high levels, all require further experimental and theoretical studies.

As the really outstanding key problems and issues related to the composition of Jupiter's atmosphere and processes affecting composition, we would nominate the following.

Firstly, the apparent low-temperature origin of the building blocks of Jupiter needs to be confirmed and explained. The key to this is the question of the bulk O/H ratio in Jupiter, which is needed to quantify the role of ice in the processes by which the planet, and the solar system, formed. A new entry probe, even if it were no more advanced than *Galileo*, could make valuable progress if deployed in a cloudy zone for contrast with the existing data from a hot spot. But the greatest advances will come from a multi-element mission with probes that reach 50 to 100 bars at a variety of locations on the planet.

Next, the detailed meteorological processes at work and all aspects of the dynamics affecting the distribution of water vapor and other compounds (such as the vertical mixing rates, and the motions and the cloud properties in the different types of giant eddies) remain mysterious in ways that have important implications for the whole subject, including terrestrial meteorology. On both planets compositional variations reveal the coupling between dynamics, chemistry, and cloud physics, but cannot at present separate and explain them, especially of course on Jupiter. For example, the distribution of water vapor, and ultimately other species, horizontally and vertically, inside 5  $\mu\text{m}$  hot spots and elsewhere, needs a great deal of clarification by new measurements using remote sensing and eventually in situ floating stations. The dynamical natures of the variously-colored giant eddies must have compositional implications, and vice-versa, that we have not really started to probe and certainly not to comprehend.

One of the oldest problems is that of the chromophores – the chemistry responsible for the coloration of the clouds on Jupiter, including those deep clouds predicted by models but yet to be seen. In the first Jupiter book, Sill (1976) wrote: "There is no conclusive proof for any hypothesis on the production of coloured material in Jupiter's clouds." This is still true: for example, cases can still be made for inorganic polysulfides or for complex organics, with no experimental basis for discriminating.

**Acknowledgements.** The authors acknowledge support as follows: Fred Taylor and Patrick Irwin from the UK Particle Physics and Astronomy Research Council, Sushil Atreya from NASA's Planetary Atmospheres Program Grant NAG 5-11004, Therese Encrenaz from the Centre National de la Recherche Scientifique (CNRS), and Tobias Owen from the NASA *Galileo* and *Cassini-Huygens* Programs.

#### REFERENCES

- Anders, E. and N. Grevesse, Abundances of the elements: Meteoritic and solar, *Geochim. Cosmochim. Acta* **53**, 197–214, 1989.
- Atkinson, D. H., J. B. Pollack, and A. Seiff, The *Galileo* probe Doppler wind experiment: Measurement of the deep zonal winds on Jupiter, *J. Geophys. Res.* **103**, 22911–22928, 1998.
- Atreya, S. and P. Romani, Photochemistry and clouds of Jupiter, Saturn, and Uranus, in *Planetary Meteorology*, G. E. Hunt, ed., pp. 17–68, Cambridge University Press, 1985.
- Atreya, S. K., *Atmospheres and Ionospheres of the Outer Planets and their Satellites*, Springer Verlag, 1986.
- Atreya, S. K., M. H. Wong, T. C. Owen, H. B. Niemann, and P. R. Mahaffy, Chemistry and clouds of the Jupiter's atmosphere: A *Galileo* perspective, in *The Three Galileos: the Man, the Spacecraft, the Telescope*, p. 249, 1997.
- Atreya, S. K., M. H. Wong, T. C. Owen, P. R. Mahaffy, H. B. Niemann, I. de Pater, P. Drossart, and T. Encrenaz, A comparison of the atmospheres of Jupiter and Saturn: Deep atmospheric composition, cloud structure, vertical mixing, and origin, *Planet. Space Sci.* **47**, 1243–1262, 1999.
- Atreya, S. K., P. R. Mahaffy, H. B. Niemann, M. H. Wong, and T. C. Owen, Composition and origin of the atmosphere of Jupiter: An update, and implications for the extrasolar giant planets, *Planet. Space Sci.* **51**, 105–112, 2003.
- Bahcall, J. N. and R. K. Ulrich, Solar models, neutrino experiments, and helioseismology, *Rev. Mod. Phys.* **60**, 297–372, 1988.
- Baines, K. H., R. W. Carlson, and L. W. Kamp, Fresh ammonia ice clouds in Jupiter: Spectroscopic identification, spatial distribution, and dynamical implications, *Icarus* **159**, 74–94, 2002.
- Basu, S. and H. M. Antia, Helium abundance in the solar envelope, *MNRAS* **276**, 1402–1408, 1995.
- Beer, R., Detection of carbon monoxide in Jupiter, *ApJ* **200**, L167–L169, 1975.
- Beer, R. and F. W. Taylor, The abundance of CH<sub>3</sub>D and the D/H ratio in Jupiter, *ApJ* **179**, 309–328, 1973.
- Beer, R. and F. W. Taylor, The abundance of carbon monoxide in Jupiter, *ApJ* **221**, 1100–1109, 1978a.
- Beer, R. and F. W. Taylor, The D/H and C/H ratios in Jupiter from the CH<sub>3</sub>D phase, *ApJ* **219**, 763–767, 1978b.
- Belton, M. J. S., J. W. Head, A. P. Ingersoll, R. Greeley, A. S. McEwen, K. P. Klaassen, D. Senke, R. Pappalardo, G. Collins, A. R. Vasavada, R. Sullivan, D. Simonelli, P. Geissler, M. H. Carr, M. E. Davies, J. Veverka, P. J. Gierasch, D. Banfield, M. Bell, C. R. Chapman, C. Anger, R. Greenberg, G. Neukum, C. B. Pilcher, R. F. Beebe, J. A. Burns, F. Fanale, W. Ip, T. V. Johnson, D. Morrison, J. Moore, G. S. Orton, P. Thomas, and R. A. West, *Galileo's* first images of Jupiter and the Galilean satellites, *Science* **274**, 377–385, 1996.
- Bergin, E. A., E. Lellouch, M. Harwit, M. A. Gurwell, G. J. Melnick, M. L. N. Ashby, G. Chin, N. R. Erickson, P. F. Goldsmith, J. E. Howe, S. C. Kleiner, D. G. Koch, D. A. Neufeld, B. M. Patten, R. Plume, R. Schieder, R. L. Snell, J. R. Stauffer, V. Tolls, Z. Wang, G. Winnewisser, and Y. F. Zhang, Submillimeter wave astronomy satellite observations of Jupiter and Saturn: Detection of 557 GHz water emission from the upper atmosphere, *ApJ* **539**, L147–L150, 2000.
- Bézar, B., E. Lellouch, D. Strobel, J. Maillard, and P. Drossart, Carbon monoxide on Jupiter: Evidence for both internal and external sources, *Icarus* **159**, 95–111, 2002.
- Bézar, B., P. Drossart, T. H. Encrenaz, and H. Fechtgruber, Benzene on the giant planets, *Icarus*, **154**, 492–500, 2001.
- Bjoraker, G. L., H. P. Larson, and V. G. Kunde, The abundance and distribution of water vapor in Jupiter's atmosphere, *ApJ* **311**, 1058–1072, 1986.

- Bodmer, R., P. Bochsler, J. Geiss, R. von Steiger, and G. Gloeckler, Solar wind helium isotopic composition from SWICS/Ulysses, *Space Sci. Rev.* **72**, 61, 1995.
- Burles, S. and D. Tytler, in *Proceedings of the Second Oak Ridge Symposium on Atomic and Nuclear Astrophysics*, P. Mezzacappa (ed.), Institute of Physics, 1998.
- Carlson, B. E., A. A. Lacis, and W. B. Rossow, The abundance and distribution of water vapor in the jovian troposphere as inferred from *Voyager* IRIS observations, *ApJ* **388**, 648–668, 1992a.
- Carlson, B. E., A. A. Lacis, and W. B. Rossow, Tropospheric gas composition and cloud structure of the jovian North Equatorial Belt, *J. Geophys. Res.* **98**, 5251–5290, 1993.
- Carlson, R., W. Smythe, K. Baines, E. Barbinis, K. Becker, R. Burns, S. Calcutt, W. Calvin, R. Clark, G. Danielson, A. Davies, P. Drossart, T. Encrenaz, F. Fanale, J. Granahan, G. Hansen, P. Herrera, C. Hibbitts, J. Hui, P. Irwin, T. Johnson, L. Kamp, H. Kieffer, F. Leader, E. Lellouch, R. Lopes-Gautier, D. Matson, T. McCord, R. Mehlman, A. Ocampo, G. Orton, M. Roos-Serote, M. Segura, J. Shirley, L. Soderblom, A. Stevenson, F. Taylor, J. Torson, A. Weir, and P. Weissman, Near-infrared spectroscopy and spectral mapping of Jupiter and the Galilean satellites: Results from *Galileo's* initial orbit, *Science* **274**, 385–388, 1996.
- Carlson, R. W., P. R. Weissman, W. D. Smythe, and J. C. Mahoney, Near-Infrared Mapping Spectrometer experiment on *Galileo*, *Space Sci. Rev.* **60**, 457–502, 1992b.
- Combes, M., J. P. Maillard, and C. de Bergh, Evidence for a telluric value of the C-12/C-13 ratio in the atmospheres of Jupiter and Saturn, *A&A* **61**, 531–537, 1977.
- Conrath, B., R. Hanel, D. Gautier, A. Marten, and G. Lindal, The helium abundance of Uranus from *Voyager* measurements, *J. Geophys. Res.* **92**, 15003–15010, 1987.
- Conrath, B. J. and D. Gautier, Saturn helium abundance: A reanalysis of *Voyager* measurements, *Icarus* **144**, 124–134, 2000.
- Conrath, B. J. and P. J. Gierasch, Retrieval of ammonia abundances and cloud opacities on Jupiter from *Voyager* IRIS spectra, *Icarus* **67**, 444–455, 1986.
- Conrath, B. J., F. M. Flasar, J. A. Pirraglia, P. J. Gierasch, and G. E. Hunt, Thermal structure and dynamics of the jovian atmosphere: II. Visible cloud features, *J. Geophys. Res.* **86**, 8769–8775, 1981.
- Conrath, B. J., D. Gautier, R. A. Hanel, and J. S. Hornstein, The helium abundance of Saturn from *Voyager* measurements, *ApJ* **282**, 807–815, 1984.
- Conrath, B. J., P. J. Gierasch, and E. A. Ustinov, Thermal structure and para hydrogen fraction on the outer planets from *Voyager* IRIS measurements, *Icarus* **135**, 501–517, 1998.
- de Pater, I. and S. T. Massie, Models of the millimeter–centimeter spectra of the giant planets, *Icarus* **62**, 143–171, 1985.
- de Pater, I., D. Dunn, P. Romani, and K. Zahnle, Reconciling *Galileo* probe data and ground-based radio observations of ammonia on Jupiter, *Icarus* **149**, 66–78, 2001.
- Drossart, P. and T. Encrenaz, The abundance of water on Jupiter from the *Voyager* IRIS data at 5 microns, *Icarus* **52**, 483–491, 1982.
- Drossart, P., T. Encrenaz, M. Combes, V. Kunde, and R. Hanel, An estimate of the PH<sub>3</sub>, CH<sub>3</sub>D, and GeH<sub>4</sub> abundances on Jupiter from the *Voyager* IRIS data at 4.5 microns, *Icarus* **49**, 416–426, 1982.
- Dyudina, U. A., A. P. Ingersoll, G. E. Danielson, K. H. Baines, R. W. Carlson, The *Galileo* NIMS, and SSI teams, interpretation of NIMS and SSI images on the jovian cloud structure, *Icarus* **150**, 219–233, 2001.
- Encrenaz, T., The planet Jupiter, *A&A Rev.* **9**, 171–219, 1999.
- Encrenaz, T., M. Combes, and Y. Zeau, The spectrum of Jupiter between 8 and 9 microns: Estimates of the Jovian C/H and D/H ratios, *A&A* **84**, 148–153, 1980.
- Encrenaz, T., T. de Graauw, S. Schaeidt, E. Lellouch, H. Feuchtgruber, D. A. Beintema, B. Bezard, P. Drossart, M. Griffin, A. Heras, M. Kessler, K. Leech, P. Morris, P. R. Roelfsema, M. Roos-Serote, A. Salama, B. Vandenbussche, E. A. Valentijn, G. R. Davis, and D. A. Naylor, First results of ISO-SWS observations of Jupiter, *A&A* **315**, L397–L400, 1996.
- Fegley, B. J. and K. Lodders, Chemical models of the deep atmospheres of Jupiter and Saturn, *Icarus* **110**, 117–154, 1994.
- Feuchtgruber, H., E. Lellouch, T. de Graauw, B. Bézard, T. Encrenaz, and M. Griffin, External supply of oxygen to the atmospheres of giant planets, *Nature* **389**, 159–162, 1997.
- Feuchtgruber, H., E. Lellouch, T. Encrenaz, B. Bézard, A. Coustenis, P. Drossart, A. Salama, T. de Graauw, and G. R. Davis, Oxygen in the stratospheres of the giant planets and Titan, in *ESA SP-427: The Universe as Seen by ISO*, vol. 427, p. 133, 1999.
- Folkner, W. M., R. Woo, and S. Nandi, Ammonia abundance in Jupiter's atmosphere derived from the attenuation of the *Galileo* probe's radio signal, *J. Geophys. Res.* **103**, 22847–22856, 1998.
- Fouchet, T., E. Lellouch, B. Bézard, T. Encrenaz, P. Drossart, H. Feuchtgruber, and T. de Graauw, ISO-SWS observations of Jupiter: Measurement of the ammonia tropospheric profile and of the <sup>15</sup>N/<sup>14</sup>N isotopic ratio, *Icarus* **143**, 223–243, 2000.
- Gautier, D. and T. Owen, The composition of outer planet atmospheres, in *Origin and Evolution of Planetary and Satellite Atmospheres*, pp. 487–512, 1989.
- Gautier, D., B. Conrath, M. Flasar, R. Hanel, V. Kunde, A. Chedin, and N. Scott, The helium abundance of Jupiter from *Voyager*, *J. Geophys. Res.* **86**, 8713–8720, 1981.
- Gautier, D., F. Hersant, O. Mousis, and J. I. Lunine, Enrichments in volatiles in Jupiter: A new interpretation of the *Galileo* measurements, *ApJ* **550**, L227–L230, 2001a.
- Gautier, D., F. Hersant, O. Mousis, and J. I. Lunine, Erratum: Enrichments in volatiles in Jupiter: A new interpretation of the *Galileo* measurements, *ApJ* **559**, L183–L183, 2001b.
- Geiss, J., Primordial abundance of hydrogen and helium isotopes, in *Origin and Evolution of the Elements*, N. Prantzos, E. Vangioni-Flam, and M. Cassè, eds, pp. 89–106, Cambridge University Press, 1993.
- Geiss, J. and G. Gloeckler, Abundances of deuterium and helium-3 in the protosolar cloud, *Space Sci. Rev.* **84**, 239–250, 1998.
- Grevesse, N. and A. J. Sauval, Standard solar composition, *Space Sci. Rev.* **85**, 161–174, 1998.
- Guillot, T., A comparison of the interiors of Jupiter and Saturn, *Planet. Space Sci.* **47**, 1183–1200, 1999.
- Holweger, H., Photospheric abundances: Problems, updates, implications, in *Joint SOHO/ACE workshop on Solar and Galactic Composition*, p. 23, 2001.
- Hubbard, W. B. and J. J. Macfarlane, Theoretical predictions of deuterium abundances in the Jovian planets, *Icarus* **44**, 676–682, 1980.
- Irwin, P. G. J., Cloud structure and composition of Jupiter's atmosphere, *Surveys Geophys.* **103**, 23001–23021, 1999.
- Irwin, P. G. J., P. Parrish, T. Fouchet, S. B. Calcutt, F. W. Taylor, A. A. Simon-Miller, and C. A. Nixon, Retrievals of jovian tropospheric phosphine from Cassini/CIRS, *Icarus*, in press, 2003.
- Irwin, P. G. J., A. L. Weir, S. E. Smith, F. W. Taylor, A. L. Lambert, S. B. Calcutt, P. J. Cameron-Smith, R. W. Carlson, K. Baines, G. S. Orton, P. Drossart, T. Encrenaz, and M. Roos-Serote, Cloud structure and atmospheric

- composition of Jupiter retrieved from *Galileo* near-infrared mapping spectrometer real-time spectra, *J. Geophys. Res.* **103**, 23 001–23 022, 1998.
- Jeffreys, H., The constitution of the four outer planets, *MNRAS* **83**, 350, 1923.
- Jeffreys, H., On the internal constitution of Jupiter and Saturn, *MNRAS* **84**, 534, 1924.
- Judge, D. L. and R. W. Carlson, *Pioneer 10* observations of the ultraviolet glow in the vicinity of Jupiter, *Science* **183**, 317–318, 1974.
- Kiess, C. C., C. H. Corliss, and H. K. Kiess, High-dispersion spectra of Jupiter, *ApJ* **132**, 221, 1960.
- Kim, S. J., J. Caldwell, A. R. Rivolo, R. Wagener, and G. S. Orton, Infrared polar brightening on Jupiter: III. Spectrometry from the *Voyager 1* IRIS experiment, *Icarus* **64**, 233–248, 1985.
- Kunde, V., R. Hanel, W. Maguire, D. Gautier, J. P. Baluteau, A. Marten, A. Chedin, N. Husson, and N. Scott, The tropospheric gas composition of Jupiter's North Equatorial Belt:  $\text{NH}_3$ ,  $\text{PH}_3$ ,  $\text{CH}_3\text{D}$ ,  $\text{GeH}_4$ ,  $\text{H}_2\text{O}$  and the jovian D/H isotopic ratio, *ApJ* **263**, 443–467, 1982.
- Larson, H. P., G. L. Bjoraker, D. S. Davis, and R. Hofmann, The jovian atmospheric window at 2.7 microns: A search for  $\text{H}_2\text{S}$ , *Icarus* **60**, 621–639, 1984.
- Lecluse, C., F. Robert, D. Gautier, and M. Guiraud, Deuterium enrichment in giant planets, *Planet. Space Sci.* **44**, 1579–1592, 1996.
- Lellouch, E., P. Drossart, and T. Encrenaz, A new analysis of the jovian 5-micron *Voyager/IRIS* spectra, *Icarus* **77**, 457–465, 1989.
- Lellouch, E., B. Bézard, R. Moreno, D. Bockelée-Morvan, P. Colom, J. Crovisier, M. Festou, D. Gautier, A. Marten, and G. Paubert, Carbon monoxide in Jupiter after the impact of Comet Shoemaker–Levy 9, *Planet. Space Sci.* **45**, 1203–1212, 1997.
- Lellouch, E., B. Bézard, T. Fouchet, H. Feuchtgruber, T. Encrenaz, and T. de Graauw, The deuterium abundance in Jupiter and Saturn from ISO-SWS observations, *A&A* **370**, 610–622, 2001.
- Lellouch, E., B. Bézard, J. I. Moses, G. R. Davis, P. Drossart, H. Feuchtgruber, E. A. Bergin, R. Moreno, and T. Encrenaz, The origin of water vapor and carbon dioxide in Jupiter's stratosphere, *Icarus* **159**, 112–131, 2002.
- Lewis, J. S., The clouds of Jupiter and the  $\text{NH}_3$ – $\text{H}_2\text{O}$  and  $\text{NH}_3$ – $\text{H}_2\text{S}$  systems, *Icarus* **10**, 365–378, 1969.
- Lindal, G. F., G. E. Wood, G. S. Levy, J. D. Anderson, D. N. Sweetnam, H. B. Hotz, B. J. Buckles, D. P. Holmes, P. E. Doms, V. R. Eshleman, G. L. Tyler, and T. A. Croft, The atmosphere of Jupiter: An analysis of the *Voyager* radio occultation measurements, *J. Geophys. Res.* **86**, 8721–8727, 1981.
- Linsky, J. L., Deuterium abundance in the local ISM and possible spatial variations, *Space Sci. Rev.* **84**, 285, 1998.
- Lodders, K. and B. Fegley, *The Planetary Scientist's Companion*, Oxford University Press, 1998.
- Lunine, J. I. and D. M. Hunten, Moist convection and the abundance of water in the troposphere of Jupiter, *Icarus* **69**, 566–570, 1987.
- Mahaffy, P. R., T. M. Donahue, S. K. Atreya, T. C. Owen, and H. B. Niemann, *Galileo* probe measurements of D/H and  $3\text{He}/4\text{He}$  in Jupiter's atmosphere, *Space Sci. Rev.* **84**, 251–263, 1998.
- Mahaffy, P. R., H. B. Niemann, A. Alpert, S. K. Atreya, J. Demick, T. M. Donahue, D. N. Harpold, and T. C. Owen, Noble gas abundance and isotope ratios in the atmosphere of Jupiter from the *Galileo* Probe Mass Spectrometer, *J. Geophys. Res.* **105**, 15 061–15 072, 2000.
- Marten, A., D. Rouan, J. P. Baluteau, D. Gautier, B. J. Conrath, R. A. Hanel, V. Kunde, R. Samuelson, A. Chedin, and N. Scott, Study of the ammonia ice cloud layer in the equatorial region of Jupiter from the infrared interferometric experiment on *Voyager*, *Icarus* **46**, 233–248, 1981.
- Massie, S. T. and D. M. Hunten, Conversion of para and ortho hydrogen in the jovian planets, *Icarus* **49**, 213–226, 1982.
- Meier, R. and T. C. Owen, Cometary deuterium, *Space Sci. Rev.* **90**, 33–43, 1999.
- Mizuno, H., Formation of the giant planets, *Prog. Theor. Phys.* **64**, 544–557, 1980.
- Niemann, H. B., S. K. Atreya, G. R. Carignan, T. M. Donahue, J. A. Haberman, D. N. Harpold, R. E. Hartle, D. M. Hunten, W. T. Kasprzak, P. R. Mahaffy, T. C. Owen, and S. H. Way, The composition of the jovian atmosphere as determined by the *Galileo* probe mass spectrometer, *J. Geophys. Res.* **103**, 22 831–22 846, 1998.
- Noll, K. S., Halogens in the giant planets: Upper limits to HBr in Saturn and Jupiter, *Icarus* **124**, 608–615, 1996.
- Noll, K. S. and H. P. Larson, The spectrum of Saturn from 1990 to 2230/cm: Abundances of  $\text{AsH}_3$ ,  $\text{CH}_3\text{D}$ ,  $\text{CO}$ ,  $\text{GeH}_4$ ,  $\text{NH}_3$ , and  $\text{PH}_3$ , *Icarus* **89**, 168–189, 1991.
- Noll, K. S., D. Gilmore, R. F. Knacke, M. Womack, C. A. Griffith, and G. Orton, Carbon monoxide in Jupiter after Comet Shoemaker–Levy 9, *Icarus* **126**, 324–335, 1997.
- Olive, K. A. and G. Steigman, On the abundance of primordial helium, *ApJS* **97**, 49–58, 1995.
- Orton, G. S. and A. P. Ingersoll, *Pioneer 10* and *11* and ground-based infrared data on Jupiter: The thermal structure and He– $\text{H}_2$  ratio, in *Jupiter*, T. Gehrels (ed), University of Arizona Press, pp. 206–215, 1976.
- Orton, G. S., J. R. Spencer, L. D. Travis, T. Z. Martin, and L. K. Tamppari, *Galileo* Photopolarimeter–Radiometer observations of Jupiter and the Galilean satellites, *Science* **274**, 389–391, 1996.
- Orton, G. S., E. Serabyn, and Y. T. Lee, Erratum to “Vertical distribution of  $\text{PH}_3$  in Saturn from observations of its 1–0 and 3–2 rotational lines,” *Icarus* **149**, 489–490, 2001.
- Owen, T. and A. Bar-Nun, Comets, impacts and atmospheres, *Icarus* **116**, 215–226, 1995.
- Owen, T., P. Mahaffy, H. B. Niemann, S. Atreya, T. Donahue, A. Bar-Nun, and I. de Pater, A low-temperature origin for the planetesimals that formed Jupiter, *Nature* **402**, 269–270, 1999.
- Owen, T., P. R. Mahaffy, H. B. Niemann, S. Atreya, and M. Wong, Protosolar nitrogen, *ApJ* **553**, L77–L79, 2001.
- Pollack, J. B., O. Hubickyj, P. Bodenheimer, J. J. Lissauer, M. Podolak, and Y. Greenzweig, Formation of the giant planets by concurrent accretion of solids and gas, *Icarus* **124**, 62–85, 1996.
- Prinn, R. G. and J. S. Lewis, Phosphine on Jupiter and implications for the Great Red Spot, *Science* **190**, 274–276, 1975.
- Roos-Serote, M., P. Drossart, T. Encrenaz, E. Lellouch, R. W. Carlson, K. H. Baines, L. Kamp, R. Mehlman, G. S. Orton, S. Calcutt, P. Irwin, F. Taylor, and A. Weir, Analysis of Jupiter North Equatorial Belt hot spots in the 4–5-micron range from *Galileo*/near-infrared mapping spectrometer observations: Measurements of cloud opacity, water, and ammonia, *J. Geophys. Res.* **103**, 23 023–23 042, 1998.
- Roos-Serote, M., P. Drossart, T. Encrenaz, R. W. Carlson, and F. Leader, Constraints on the tropospheric cloud structure of Jupiter from spectroscopy in the 5- $\mu\text{m}$  region: A comparison between *Voyager/IRIS*, *Galileo*-NIMS, and ISO-SWS spectra, *Icarus* **137**, 315–340, 1999.
- Roos-Serote, M., A. R. Vasavada, L. Kamp, P. Drossart, P. Irwin, C. Nixon, and R. W. Carlson, Proximate humid and dry

- regions in Jupiter's atmosphere indicate complex local meteorology, *Nature* **405**, 158–160, 2000.
- Rutherford, L. M., Astronomical observations with the spectroscope, *Amer. J. Sci.* **85**, 71–77, 1863.
- Sada, P. V., G. H. McCabe, G. L. Bjoraker, D. E. Jennings, and D. C. Reuter,  $^{13}\text{C}$ -ethane in the atmospheres of Jupiter and Saturn, *ApJ* **472**, 903, 1996.
- Showman, A. P., Hydrogen halides on Jupiter and Saturn, *Icarus* **152**, 140–150, 2001.
- Sill, G. T., The chemistry of the jovian cloud colors, in *Jupiter*, T. Gehrels (ed), University of Arizona Press, pp. 372–383, 1976.
- Simon-Miller, A. A., B. Conrath, P. J. Gierasch, and R. F. Beebe, A detection of water ice on Jupiter with *Voyager* IRIS, *Icarus* **145**, 454–461, 2000.
- Simon-Miller, A. A., D. Banfield, and P. J. Gierasch, An HST study of jovian chromophores, *Icarus* **149**, 94–106, 2001.
- Spinrad, H. and L. M. Trafton, High dispersion spectra of the outer planets: I. Jupiter in the visual and red, *Icarus* **2**, 19, 1963.
- Sromovsky, L. A., A. D. Collard, P. M. Fry, G. S. Orton, M. T. Lemmon, M. G. Tomasko, and R. S. Freedman, *Galileo* probe measurements of thermal and solar radiation fluxes in the jovian atmosphere, *J. Geophys. Res.* **103**, 22 929–22 978, 1998.
- Stevenson, D. J. and E. E. Salpeter, Interior models of Jupiter, in *Jupiter*, T. Gehrels (ed) University of Arizona Press, pp. 85–112, 1976.
- Strobel, D. F.,  $\text{NH}_3$  and  $\text{PH}_3$  photochemistry in the jovian atmosphere, *ApJ* **214**, L97–L99, 1977.
- Trauger, J. T., F. L. Roesler, N. P. Carleton, and W. A. Traub, Observation of HD on Jupiter and the D/H ratio, *ApJ* **184**, L137+, 1973.
- von Zahn, U., D. M. Hunten, and G. Lehmacher, Helium in Jupiter's atmosphere: Results from the *Galileo* probe helium interferometer experiment, *J. Geophys. Res.* **103**, 22 815–22 830, 1998.
- Weidenschilling, S. J. and J. S. Lewis, Atmospheric and cloud structures of the jovian planets, *Icarus* **20**, 465–476, 1973.
- Weisstein, E. W. and E. Serabyn, Submillimeter line search in Jupiter and Saturn, *Icarus* **123**, 23–36, 1996.
- West, R. A., D. F. Strobel, and M. G. Tomasko, Clouds, aerosols, and photochemistry in the jovian atmosphere, *Icarus* **65**, 161–217, 1986.
- Wong, M. H., S. K. Atreya, P. R. Mahaffy, H. B. Niemann, and T. C. Owen, Comparison of updated *Galileo* probe entry site condensable volatile profiles with the entraining downdraft model, *Icarus* **submitted**.
- Young, A. T., What color is the solar system?, *S&T* **69**, 399–402, 1985.